ATLAS measurements of Higgs boson properties in bosonic decay channels

Eleonora Benhar Noccioli
Université de Genève

on behalf of the ATLAS collaboration

PANIC 14 - Hamburg 25-29 August

SM Higgs boson production @LHC

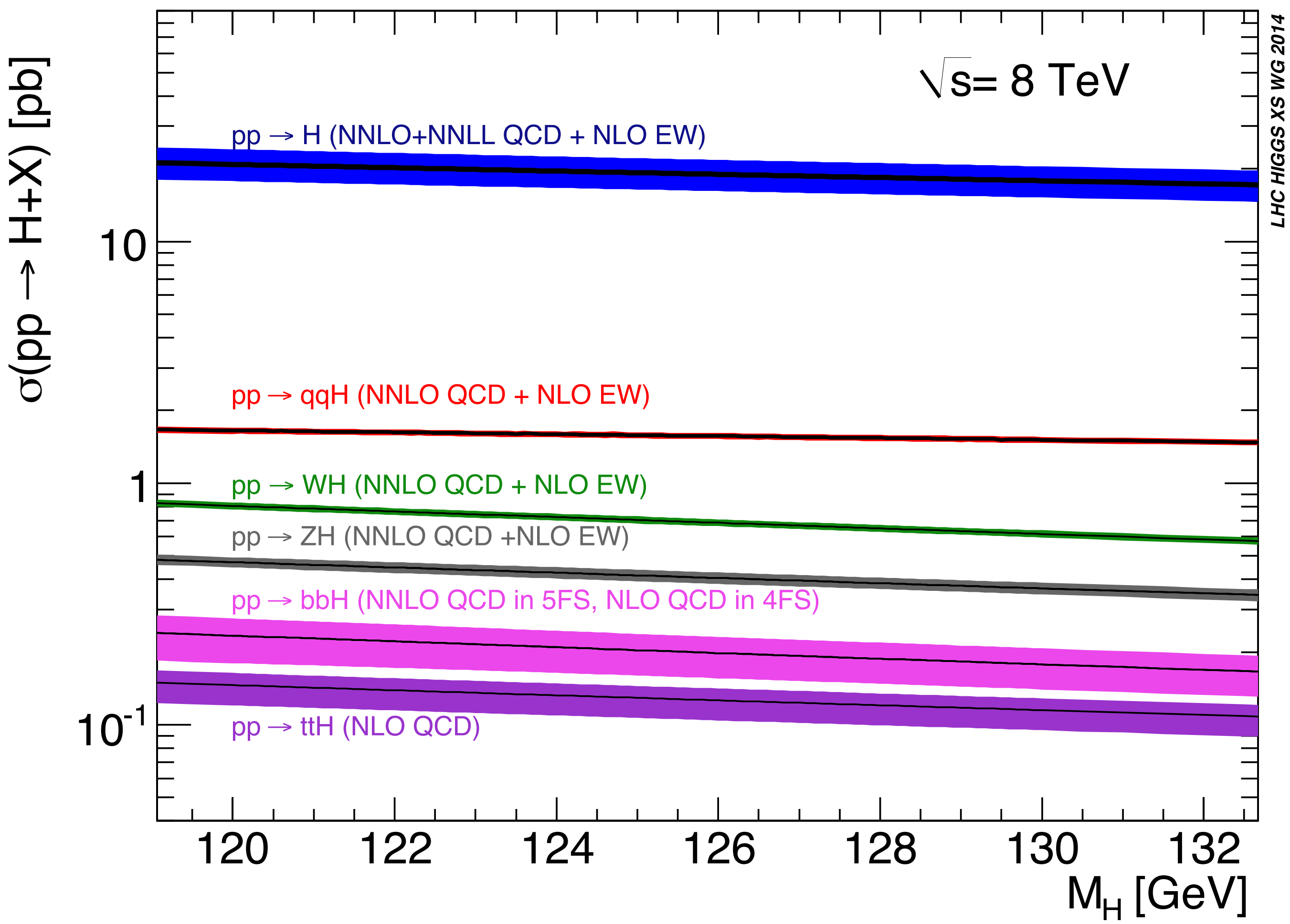

Numbers for:
$m_H = 125$ GeV
$\sqrt{s} = 8$ TeV

Gluon Fusion

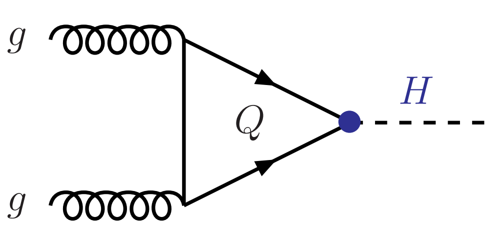

σ = 19.5 pb (87%)

Vector Boson Fusion

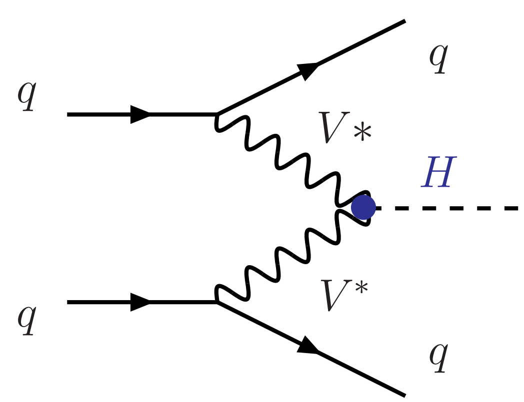

σ = 1.58 pb (7%)

Associated prod. W/Z

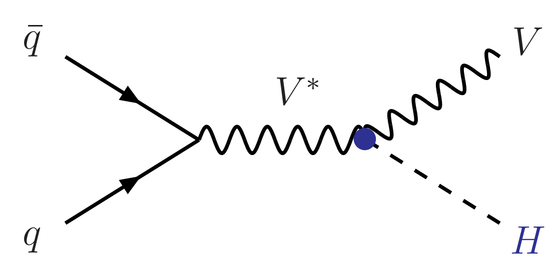

σ = 1.09 pb (5%)

Associated prod. tt/bb

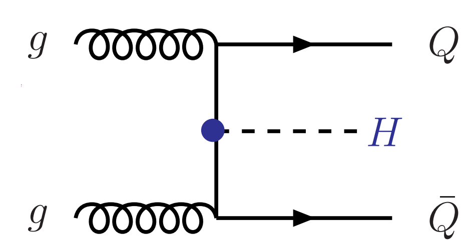

σ = 0.34 pb (1%)

SM Higgs boson decay channels

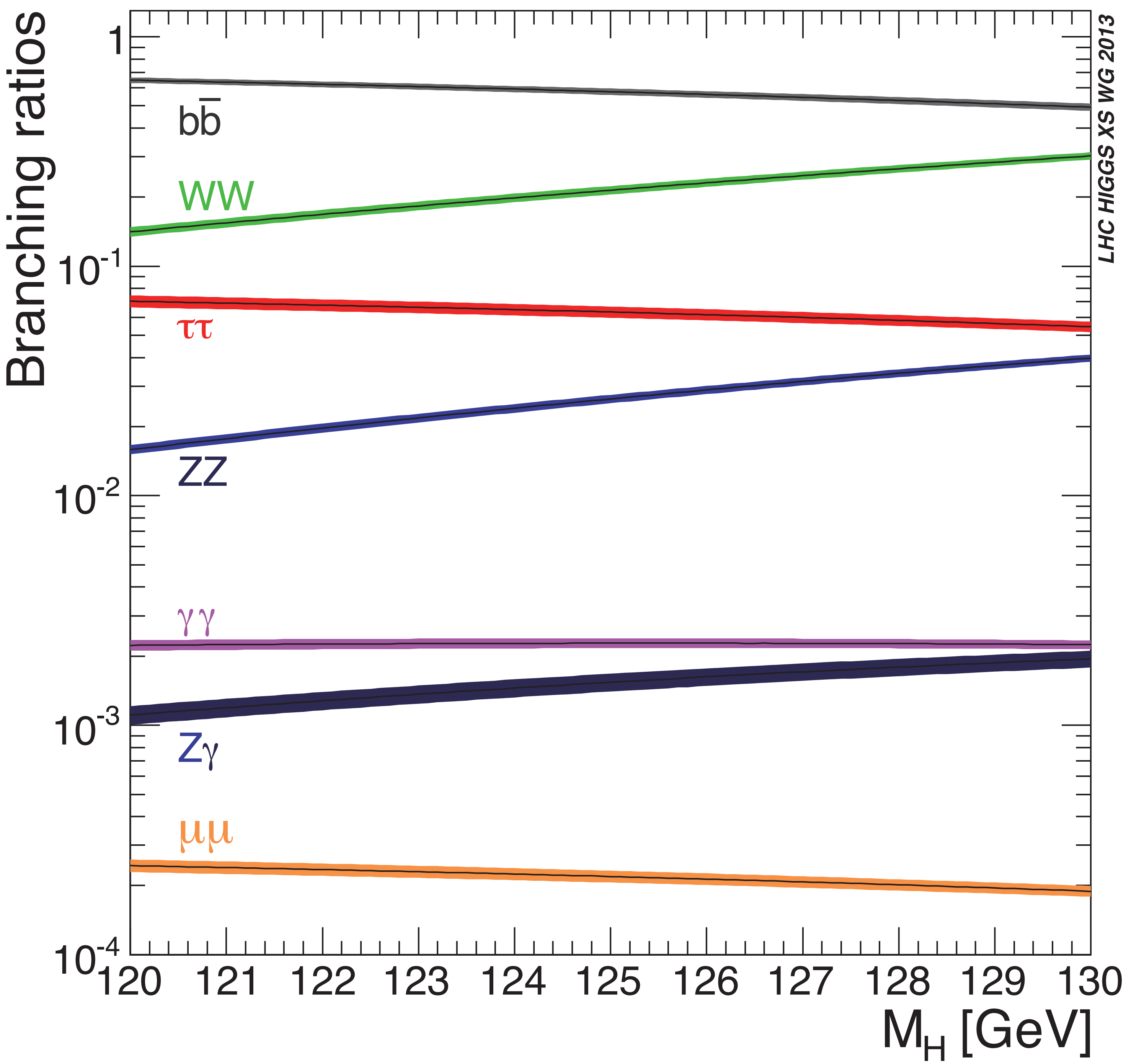

Many decay channels accessible
@ $m_H = 125$ GeV!

In this talk focus on bosonic final states:

$H \to ZZ \to 4\ell$

$H \to \gamma\gamma$

$H \to WW \to \ell\ell\nu\nu$

$H \to Z\gamma \to \ell\ell\gamma$

with emphasis on most recent results

H → ZZ → 4ℓ

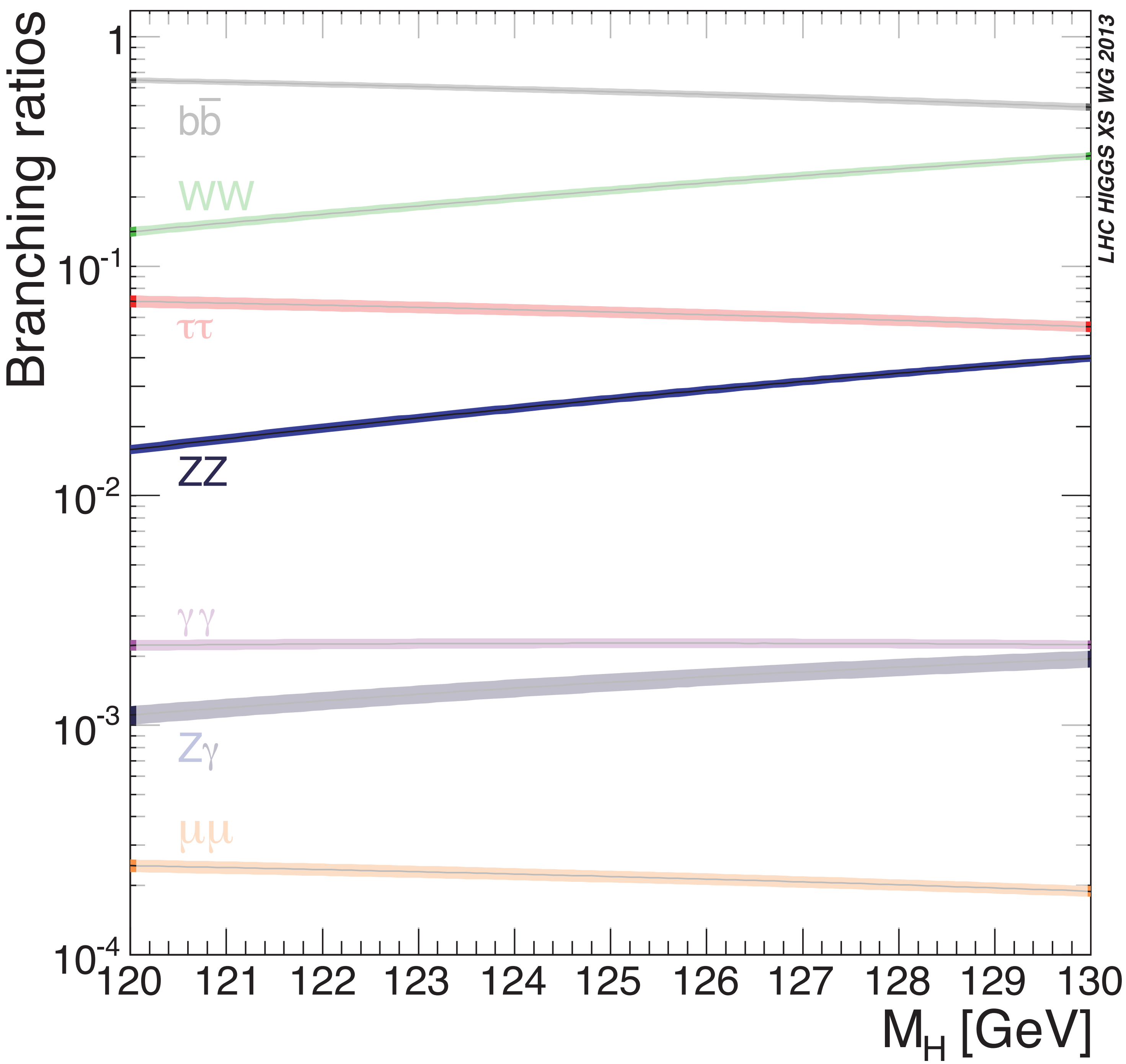

Highlights

- S/B ~ 2 in mass window 120–130 GeV
- Excellent mass resolution: 1.6 (2.2) GeV for 4μ (4e) final state
- Very low $\sigma \cdot BR$ ~ 2.9 fb for m_H=125.5 GeV @ 8 TeV

Latest public results

- Mass: arXiv 1406.3827 accepted by PRD
- Couplings: to be submitted to PRD
- Differential Cross-Sections: ATLAS-CONF-2014-044 / paper to be submitted to PRD
- Indirect Γ_H : ATLAS-CONF-2014-042
- Spin/CP: Phys. Lett. B726 (2013) 120

$H \rightarrow ZZ \rightarrow 4\ell$ analysis

NEW

- Search for peak in $m_{4\ell}$ spectrum over smooth background
- Main backgrounds: $ZZ^{(*)}$, Z+jets, ttbar
- Event selection:
  - 2 same flavor, opposite-sign lepton pairs
  - p_T>7(6) GeV for muons (electrons)
  - isolated leptons from same vertex
  - leading $m_{\ell\ell}$ (+FSR) constrained to m_Z

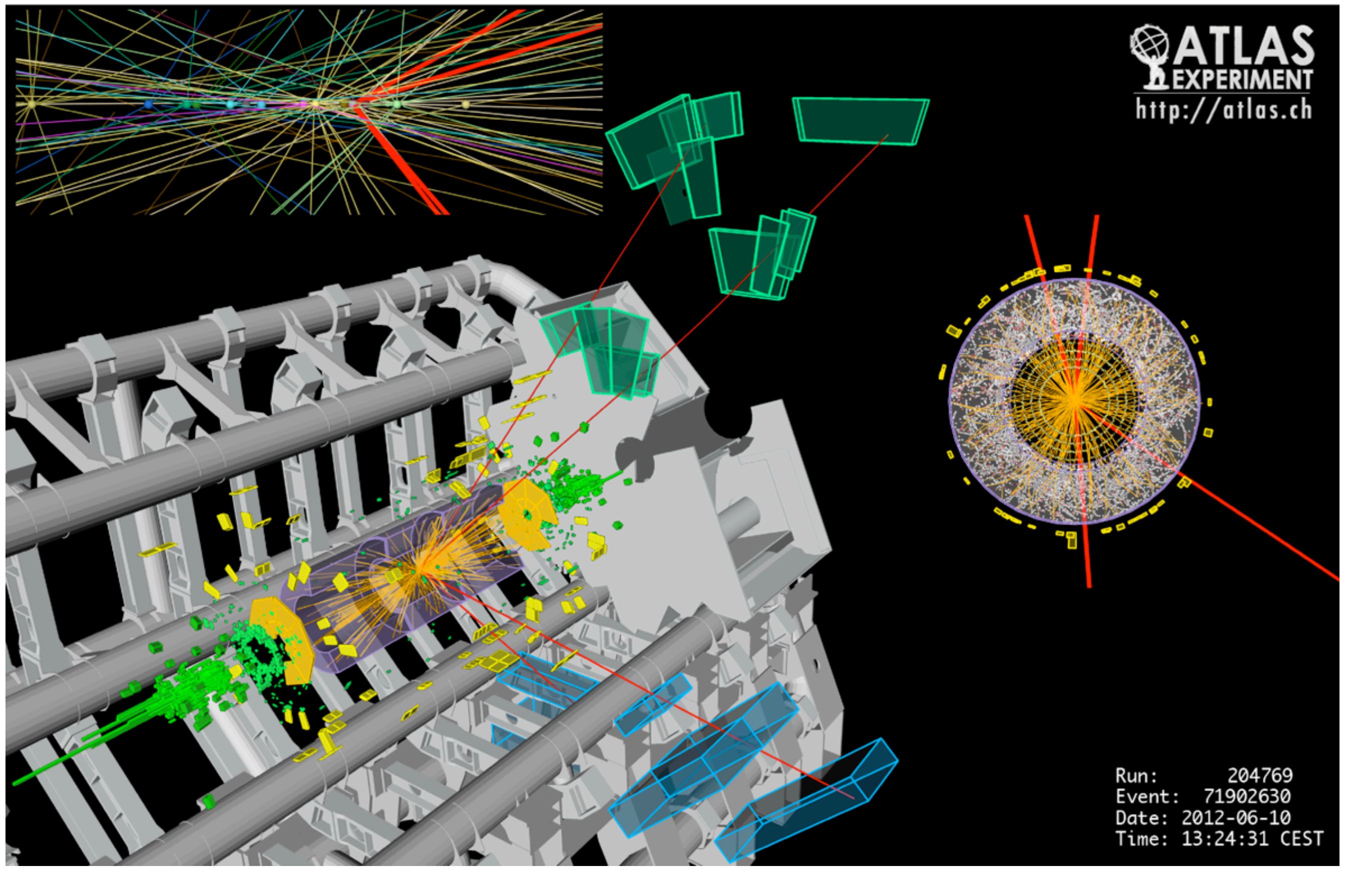

events $120 < m_{4l} < 130$ GeV

Final state	Signal full mass range	Signal	ZZ^*	Z + jets, $t\bar{t}$	s/b	Expected	Observed
	$110 < m_{4l} < 140$ GeV	$\sqrt{s}$ = 7 TeV and $\sqrt{s}$ = 8 TeV					
4μ	6.80 ± 0.67	6.20 ± 0.61	2.82 ± 0.14	0.79 ± 0.13	1.7	9.81 ± 0.64	14
$2e2\mu$	4.58 ± 0.45	4.04 ± 0.40	1.99 ± 0.10	0.69 ± 0.11	1.5	6.72 ± 0.42	9
$2\mu 2e$	3.56 ± 0.36	3.15 ± 0.32	1.38 ± 0.08	0.72 ± 0.12	1.5	5.24 ± 0.35	6
$4e$	3.25 ± 0.34	2.77 ± 0.29	1.22 ± 0.08	0.76 ± 0.11	1.4	4.75 ± 0.32	8
Total	18.2 ± 1.8	16.2 ± 1.6	7.41 ± 0.40	2.95 ± 0.33	1.6	26.5 ± 1.7	37

H→ZZ→4ℓ analysis

NEW

- Recent improvements in analysis:
  - Likelihood based electron identification
  - Electron/muon calibration
  - BDT for $ZZ^{(*)}$ suppression: matrix element kinematic discriminant + p_{4l} + η_{4l}

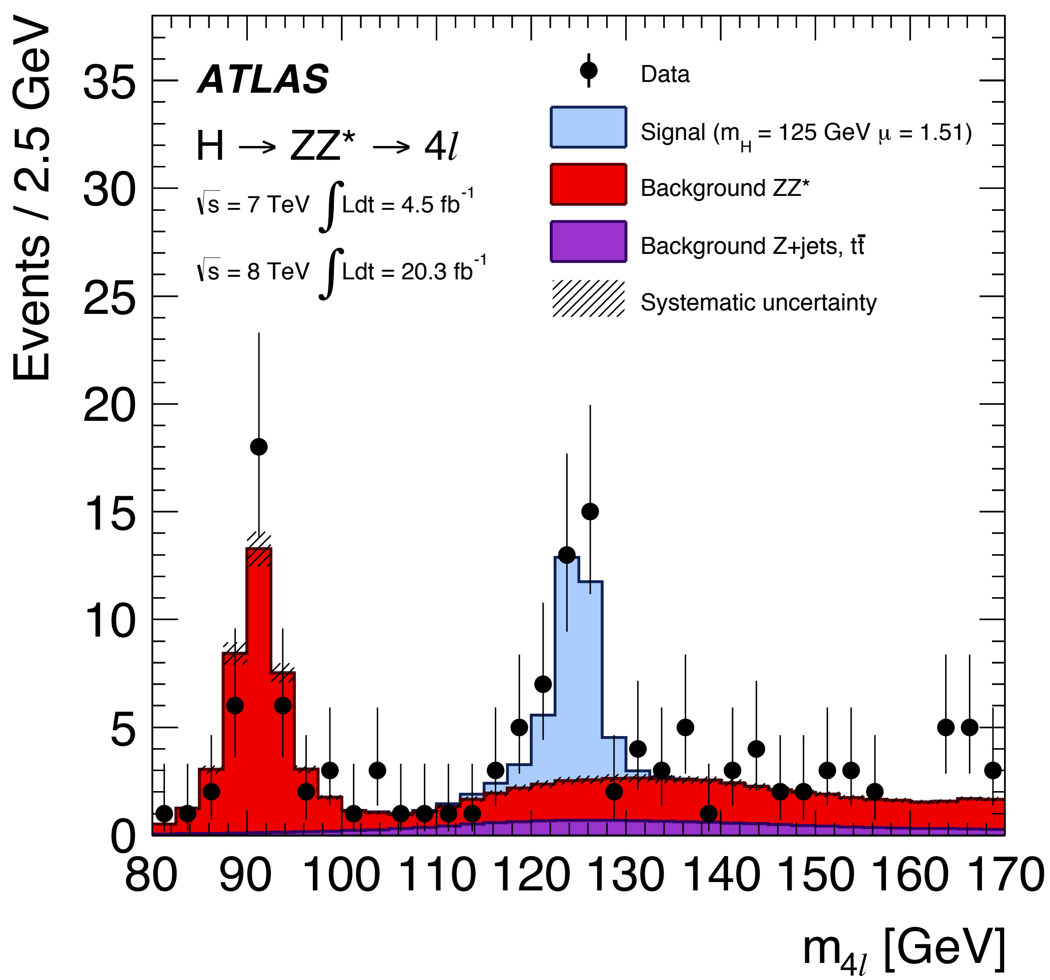

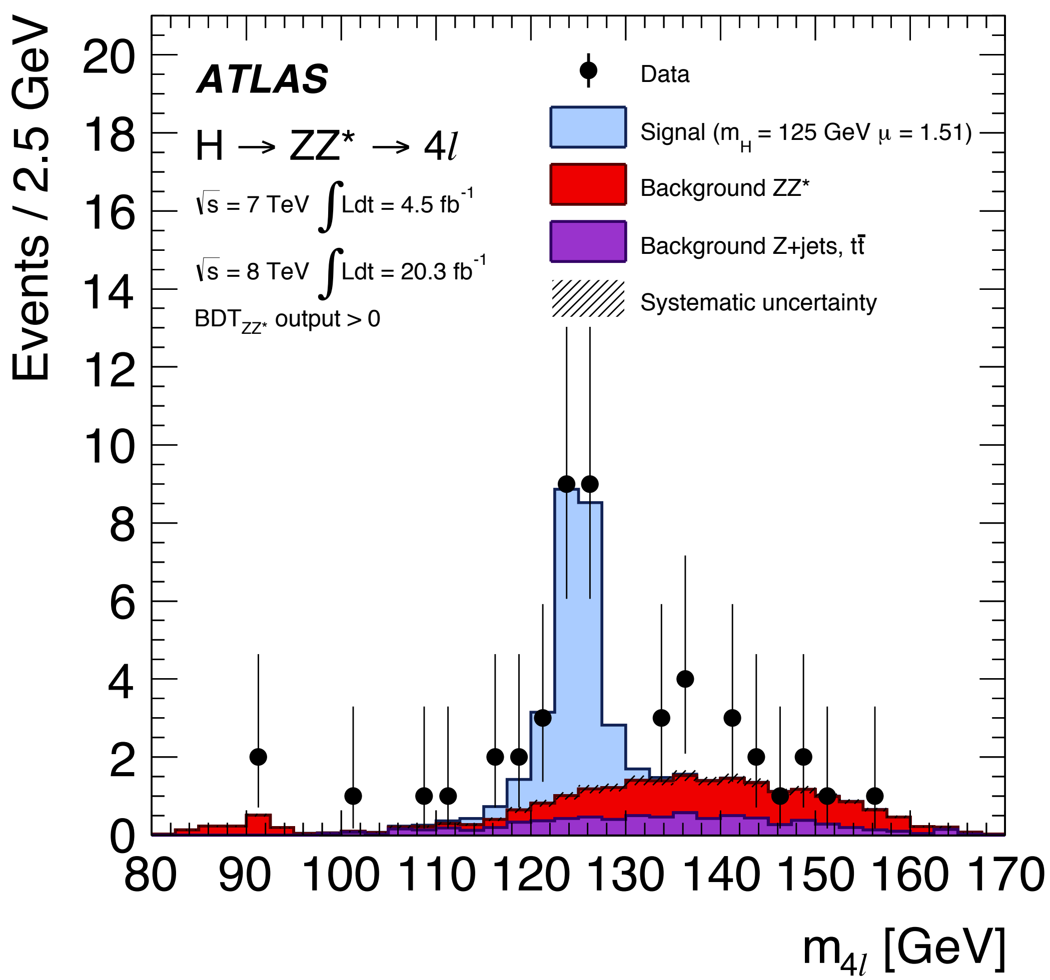

$H \to ZZ \to 4\ell$: mass measurement

NEW

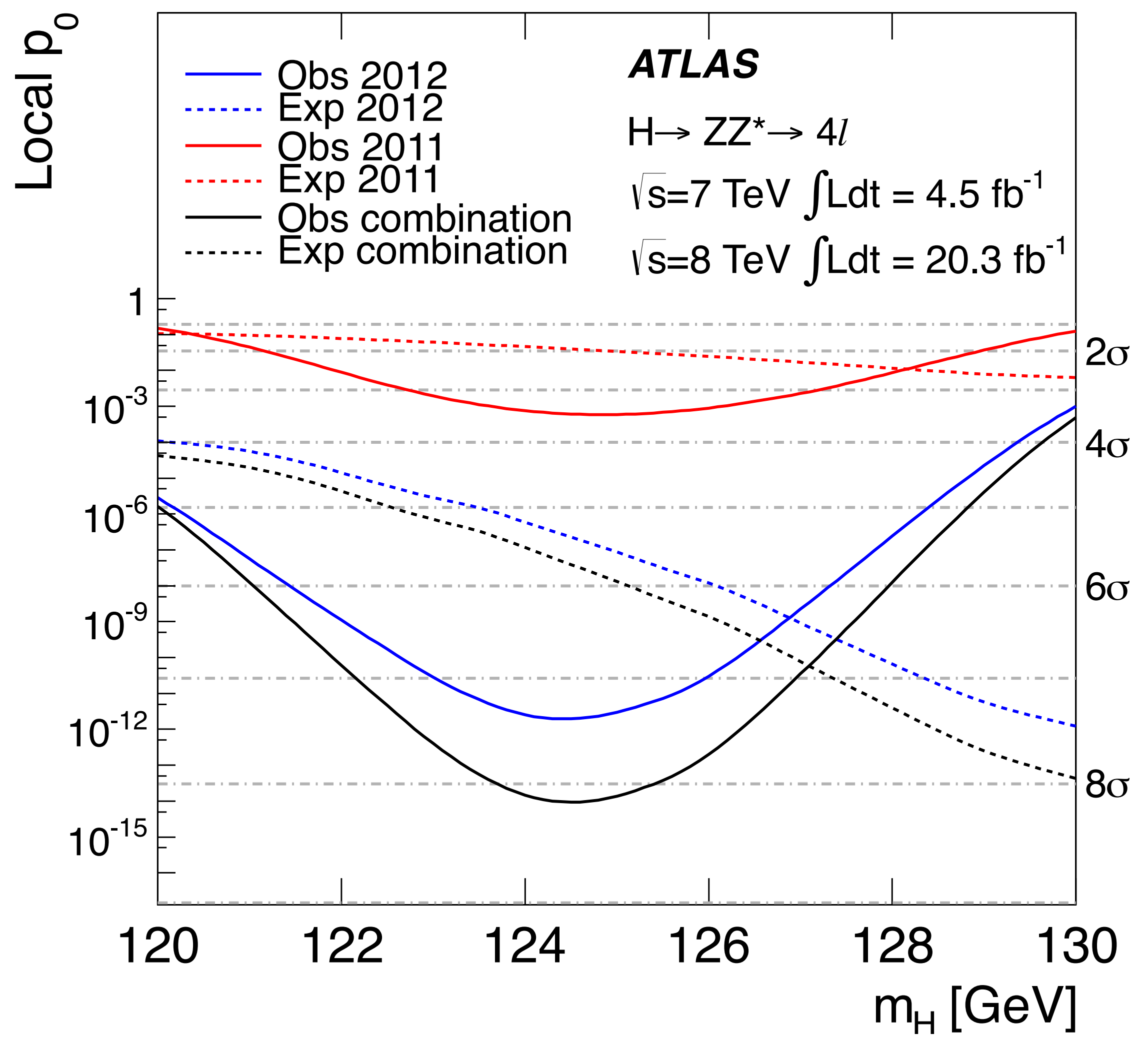

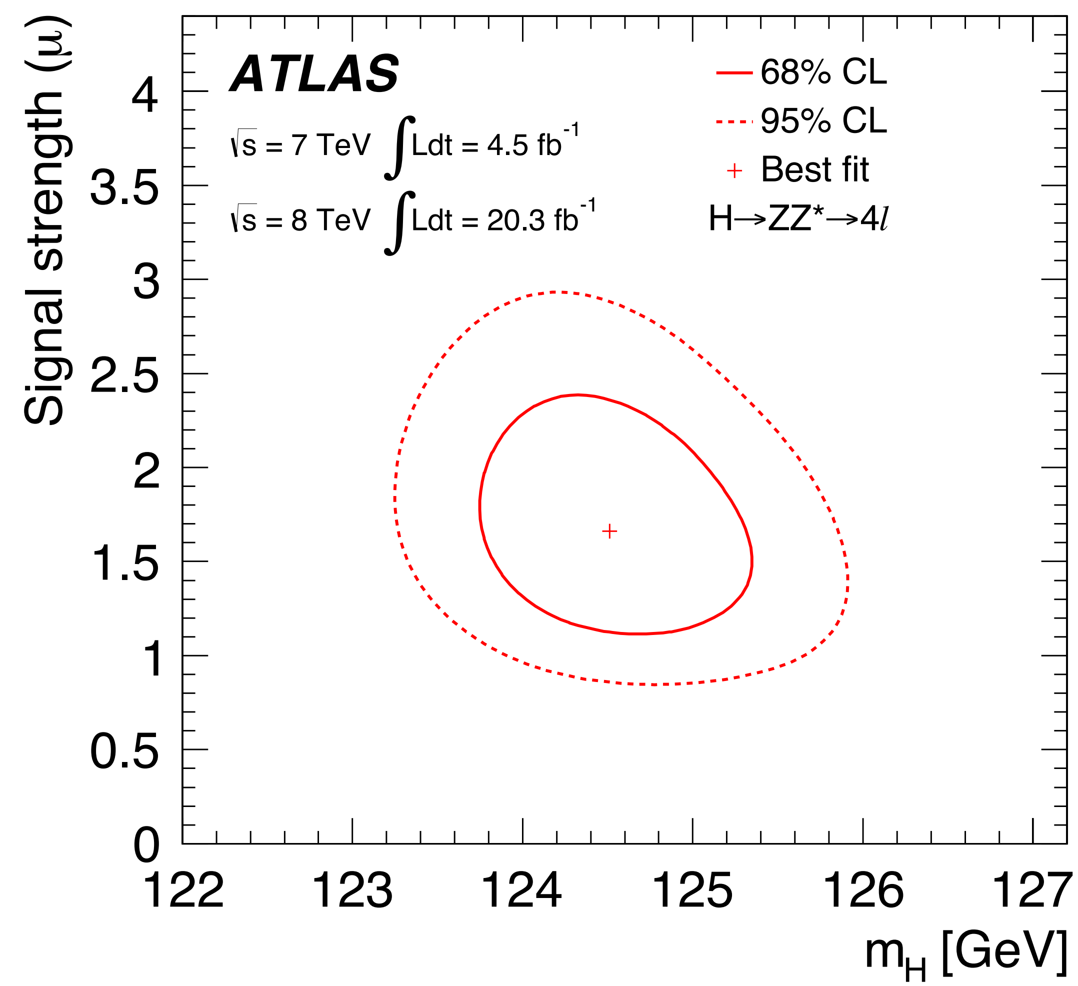

- Mass and signal strength measurement performed with 2D fit to $m_{4\ell}$ and BDT_{ZZ} (8% improvement over simple 1D fit to $m_{4\ell}$)
- Maximum local significance (at m_H=124.51): expected: 5.8σ / observed: 8.2σ

$m_H = 124.51 \pm 0.52\ (stat) \pm 0.06\ (syst)$ GeV $\qquad \mu = 1.66^{+0.45}_{-0.38}$ (at $m_H = 124.51$)

$H \to ZZ \to 4\ell$: event categories

NEW

- Events categorized according to production mechanism
  - **VBF** : $n_{Jets} \geq 2$, $m_{JJ} > 130$ GeV (2D fit to $m_{4\ell}$ and BDT_{VBF})
  - **VH hadronic** : $n_{Jets} \geq 2$, $m_{JJ} < 130$ GeV and selected by BDT_{VH} (1D fit to $m_{4\ell}$)
  - **VH leptonic** : additional lepton in event (1D fit to $m_{4\ell}$)
  - **ggF** : all other events (2D fit to $m_{4\ell}$ and BDT_{ZZ})

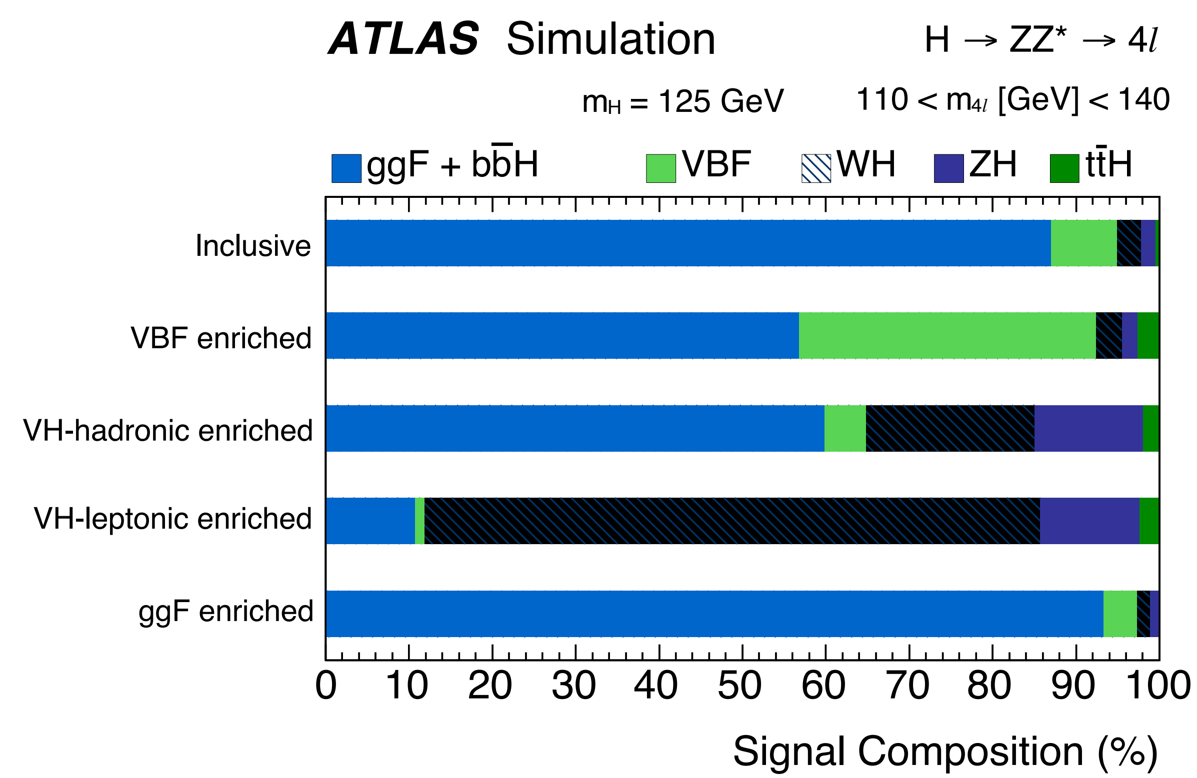

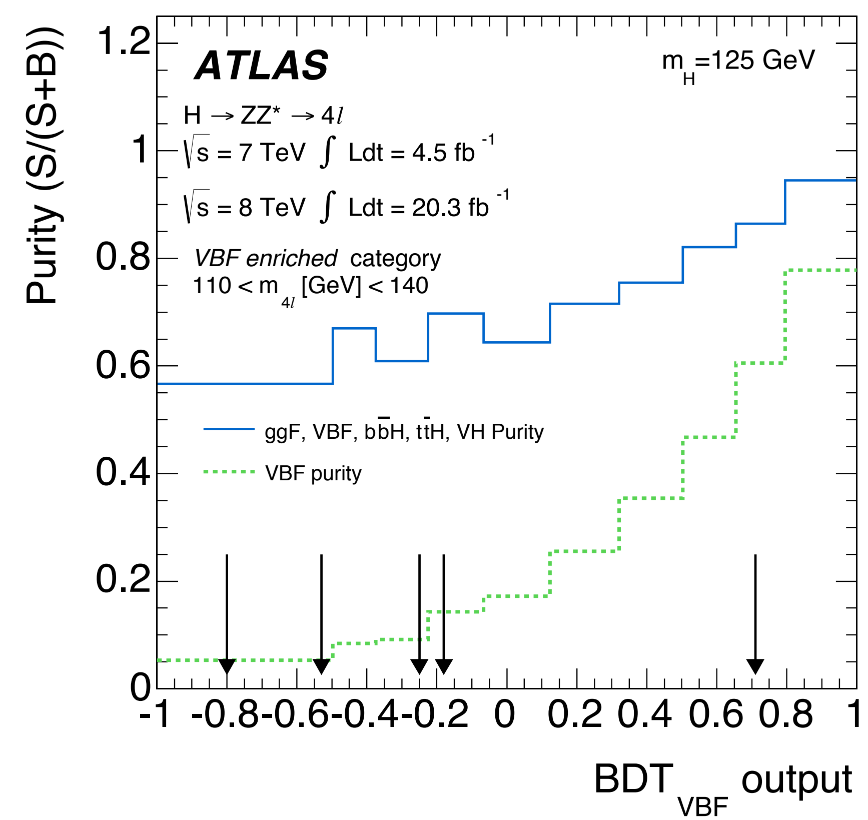

- Event yields for $m_{4\ell}$ in 110-140 GeV range:
  - no events in VH categories
  - 5 events in VBF enriched category (1 with BDT > 0)

H→ZZ→4ℓ : couplings measurement NEW

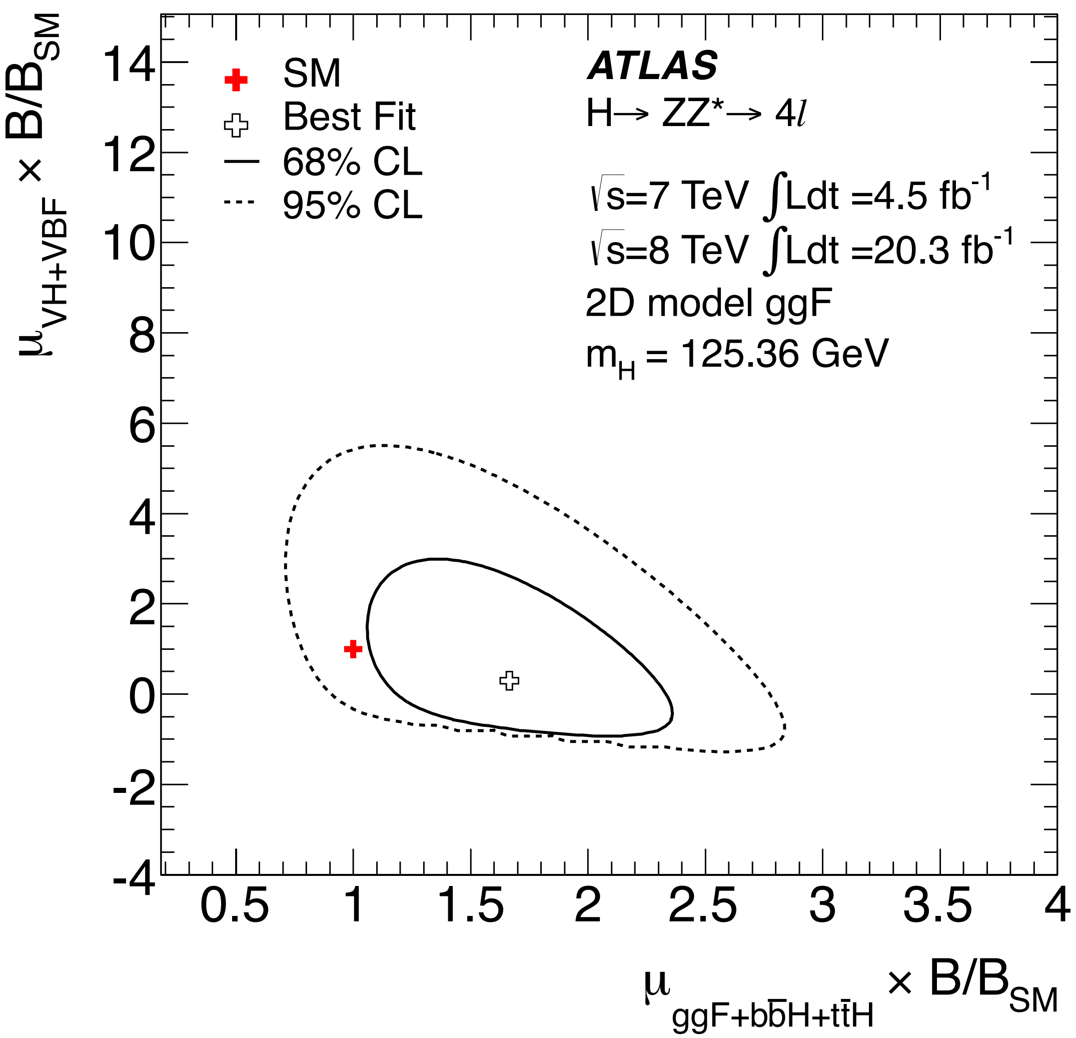

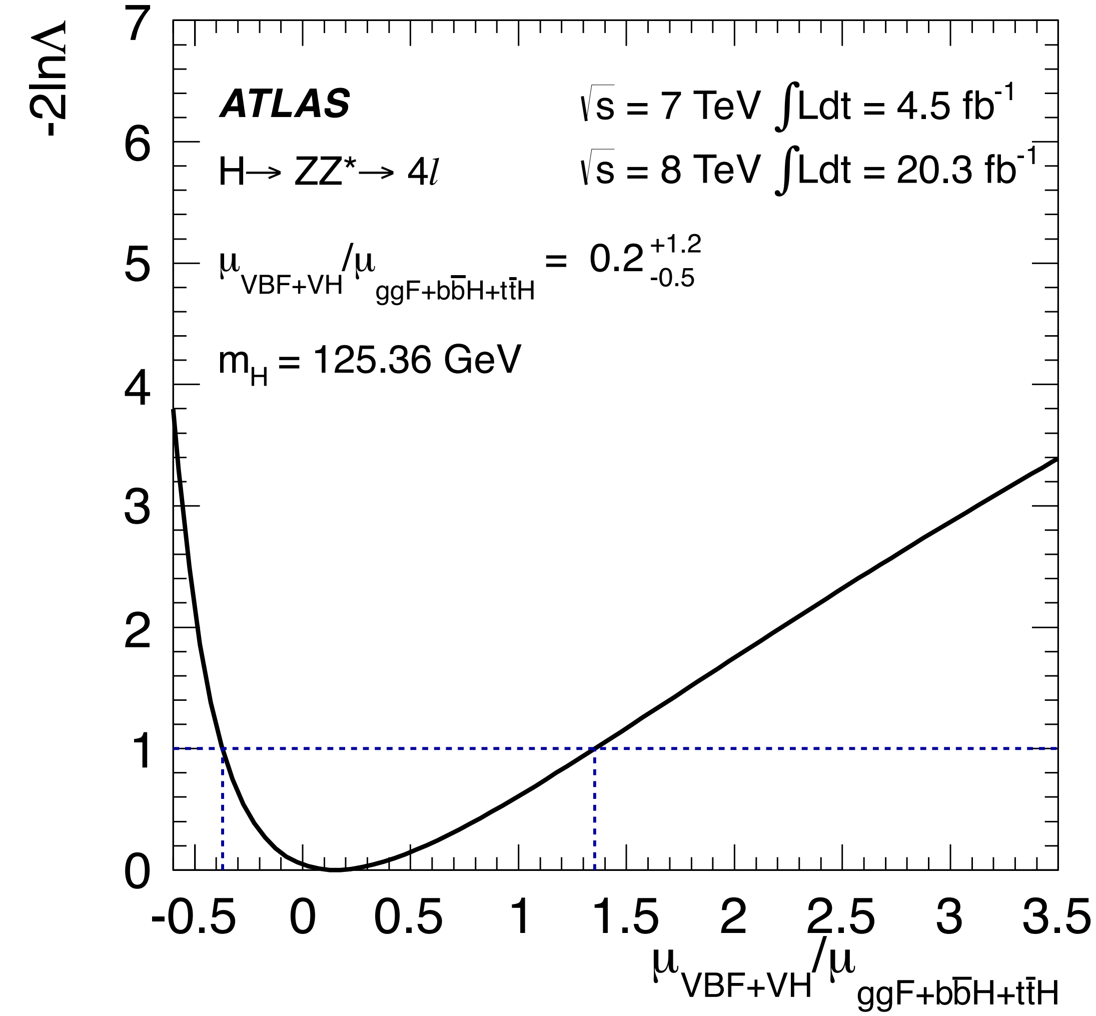

$$\mu_{ggF+bbH+ttH} = 1.66\ ^{+0.45}_{-0.41}\ (\text{stat})\ ^{+0.25}_{-0.15}\ (\text{syst})$$

$$\mu_{VBF+VH} = 0.26\ ^{+1.60}_{-0.91}\ (\text{stat})\ ^{+0.36}_{-0.23}\ (\text{syst})$$

$$\mu_{VBF+VH} / \mu_{ggF+bbH+ttH} = 0.2\ ^{+1.2}_{-0.5}$$

$H \rightarrow ZZ \rightarrow 4\ell$: fiducial cross section

NEW

$$\sigma^{tot}_{fid} = 2.11\ ^{+0.53}_{-0.47}\ \text{(stat)}\ ^{+0.08}_{-0.08}\ \text{(syst) fb}$$

$$\sigma^{exp} = 1.30 \pm 0.13\ \text{fb}$$

- Inclusive measurement with $m_{4\ell}$ fit
- 6 differential measurements
  - Higgs p_T and $|y|$, $\cos(\theta^*)$, M_{34}, N_{jets}, leading jet pT
  - cut and count method, with bin-by-bin unfolding

Variable	p-values POWHEG	MINLO	HRES2
$p_{T,H}$	0.30	0.23	0.16
$\lvert y_H \rvert$	0.37	0.45	0.36
m_{34}	0.48	0.60	-
$\lvert\cos\theta^*\rvert$	0.35	0.45	-
n_{jets}	0.37	0.28	-
p_T^{jet}	0.33	0.26	-

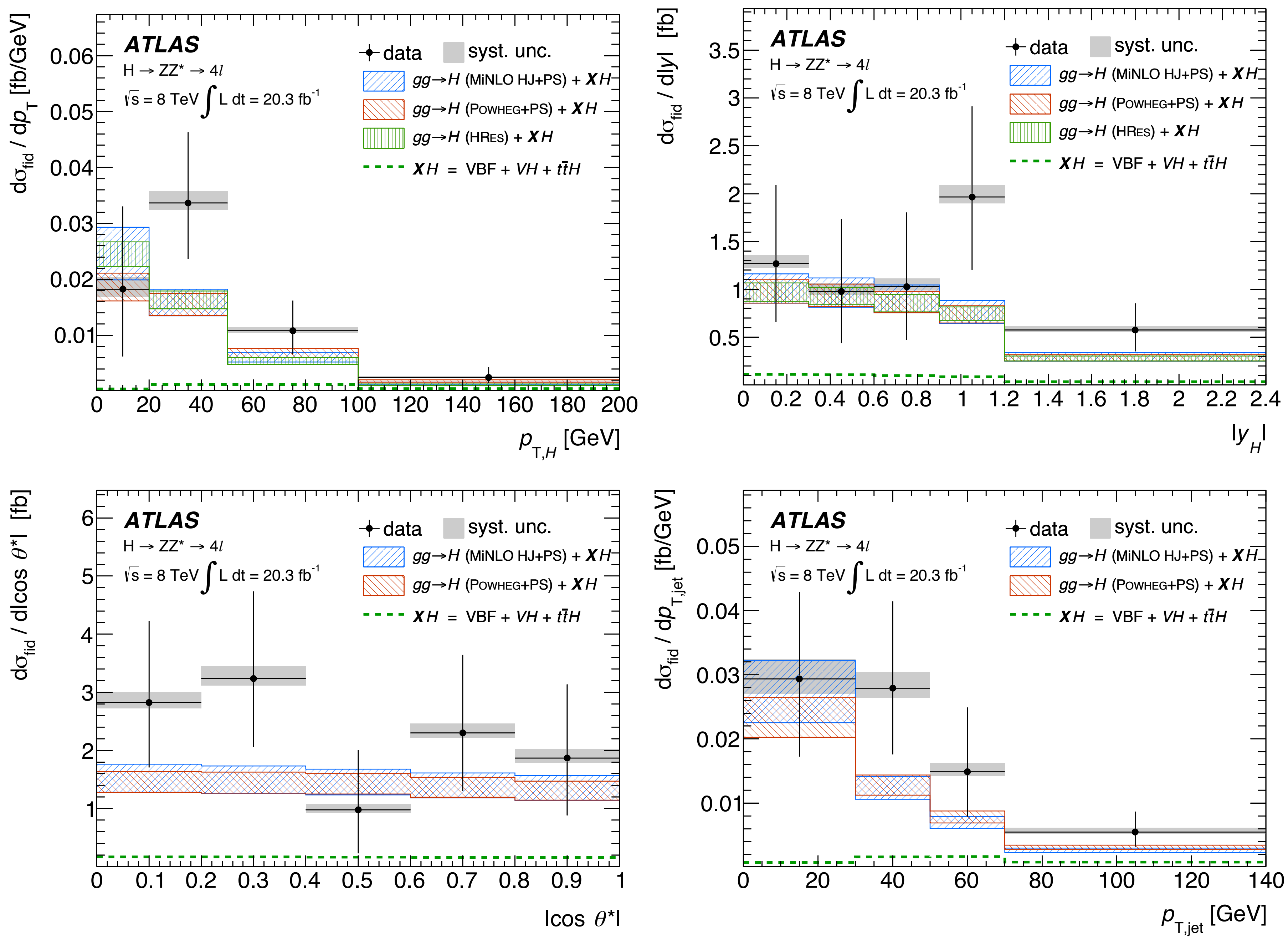

No significant deviations from theoretical predictions observed

H→ZZ: indirect Γ_H measurement

NEW

- High-mass off-peak region of H→ZZ (above $2m_Z$) sensitive to Higgs production through signal (off-shell) and background interference effects

$$\mu_{\text{on-shell}} = \frac{\kappa^2_{g,\text{on-shell}} \cdot \kappa^2_{V,\text{on-shell}}}{\Gamma_H/\Gamma_H^{\text{SM}}}$$

$$\mu_{\text{off-shell}} = \kappa^2_{g,\text{off-shell}} \cdot \kappa^2_{V,\text{off-shell}}$$

- Required assumptions:
  - SM backgrounds not sensitive to new physics modifying off-shell couplings
  - $\kappa^i_{\text{on-shell}} = \kappa^i_{\text{off-shell}}$
- gg→ZZ *K*-factors not known in off-shell region (for signal available at NNLO)

ZZ→4l
- off-peak region: 220 GeV-1 TeV
- Matrix element kinematic discriminant used to set limit

ZZ→2l2ν
- E_T^{miss} >150 GeV, 76<$m_{\ell\ell}$<106 GeV
- off-peak region m_T >350 GeV
- off-shell rate limit based on event counting

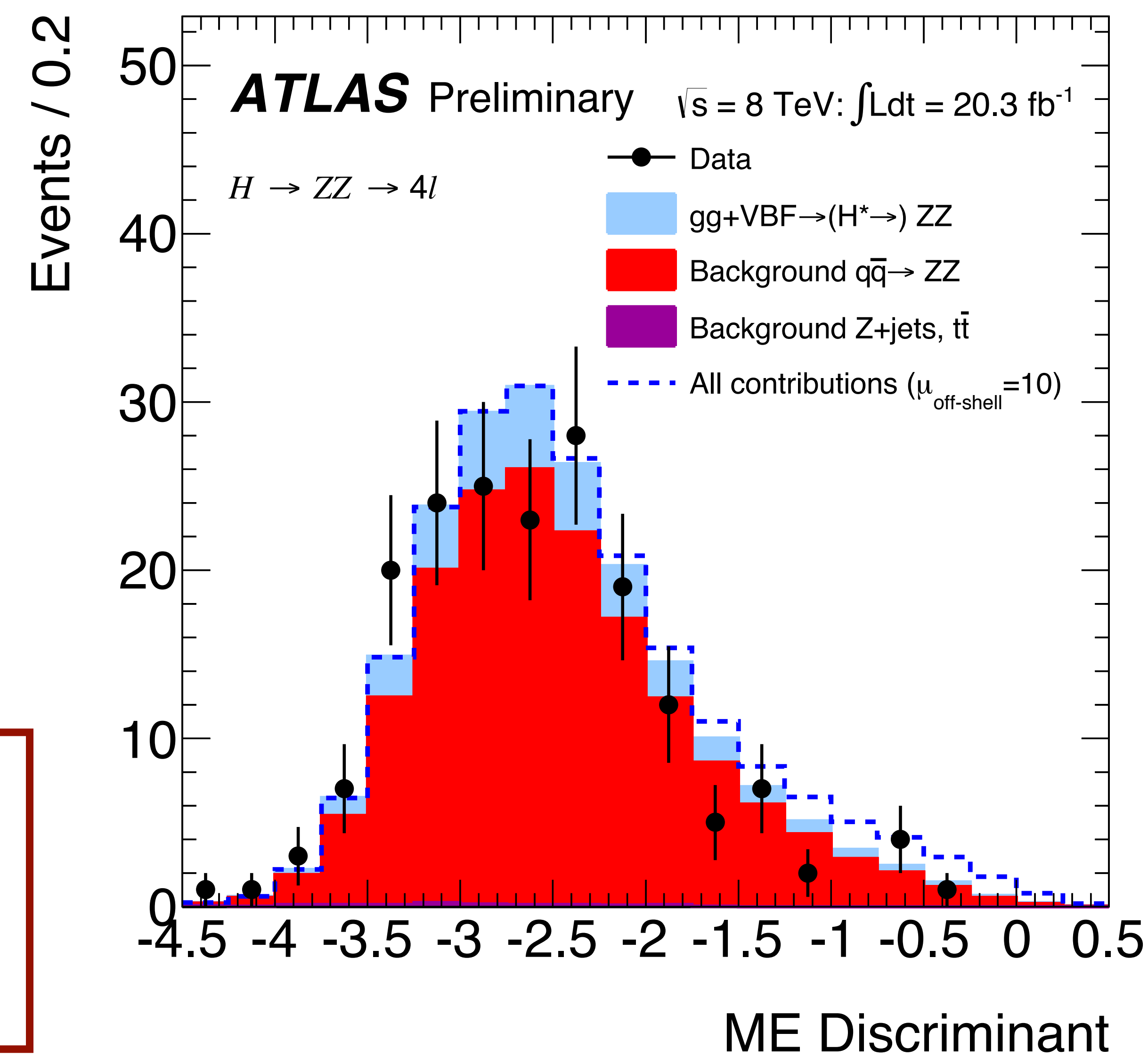

H→ZZ: indirect Γ_H measurement

NEW

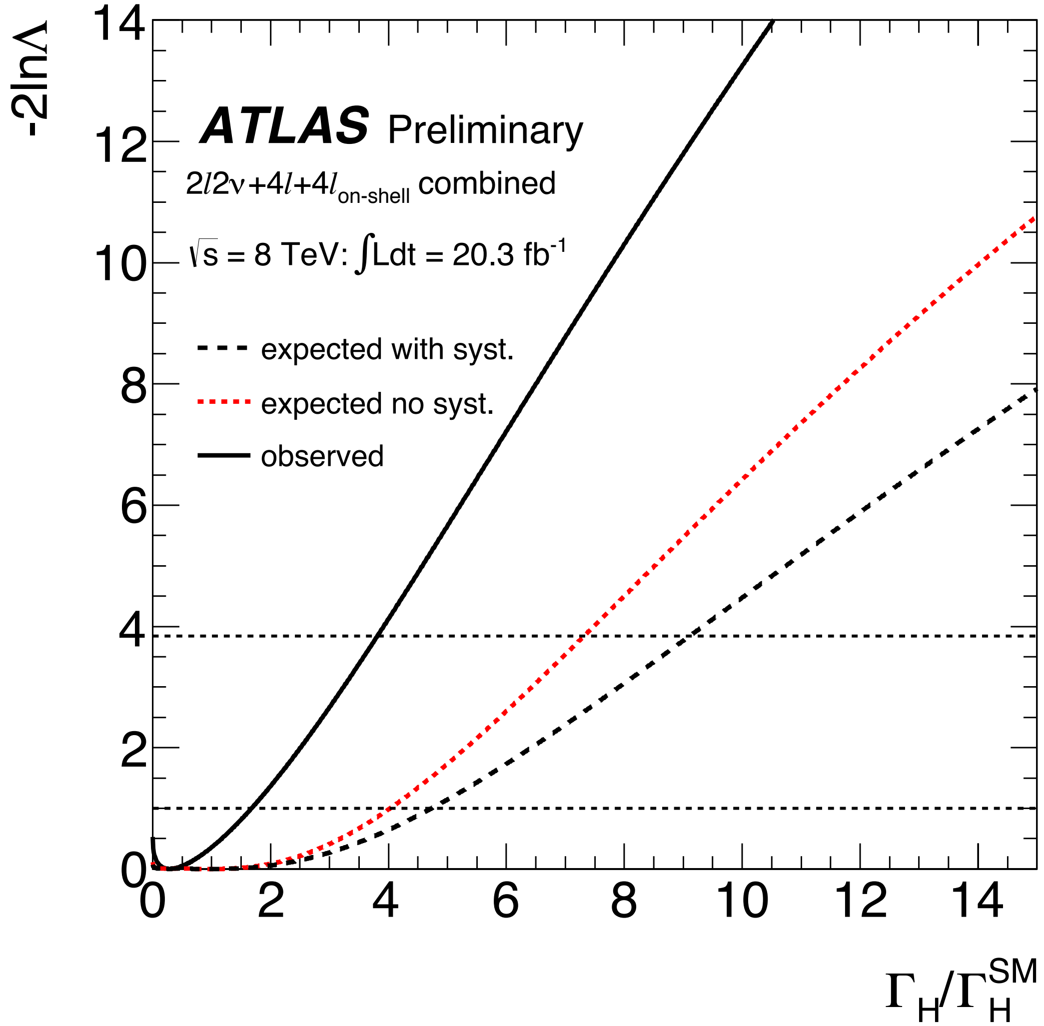

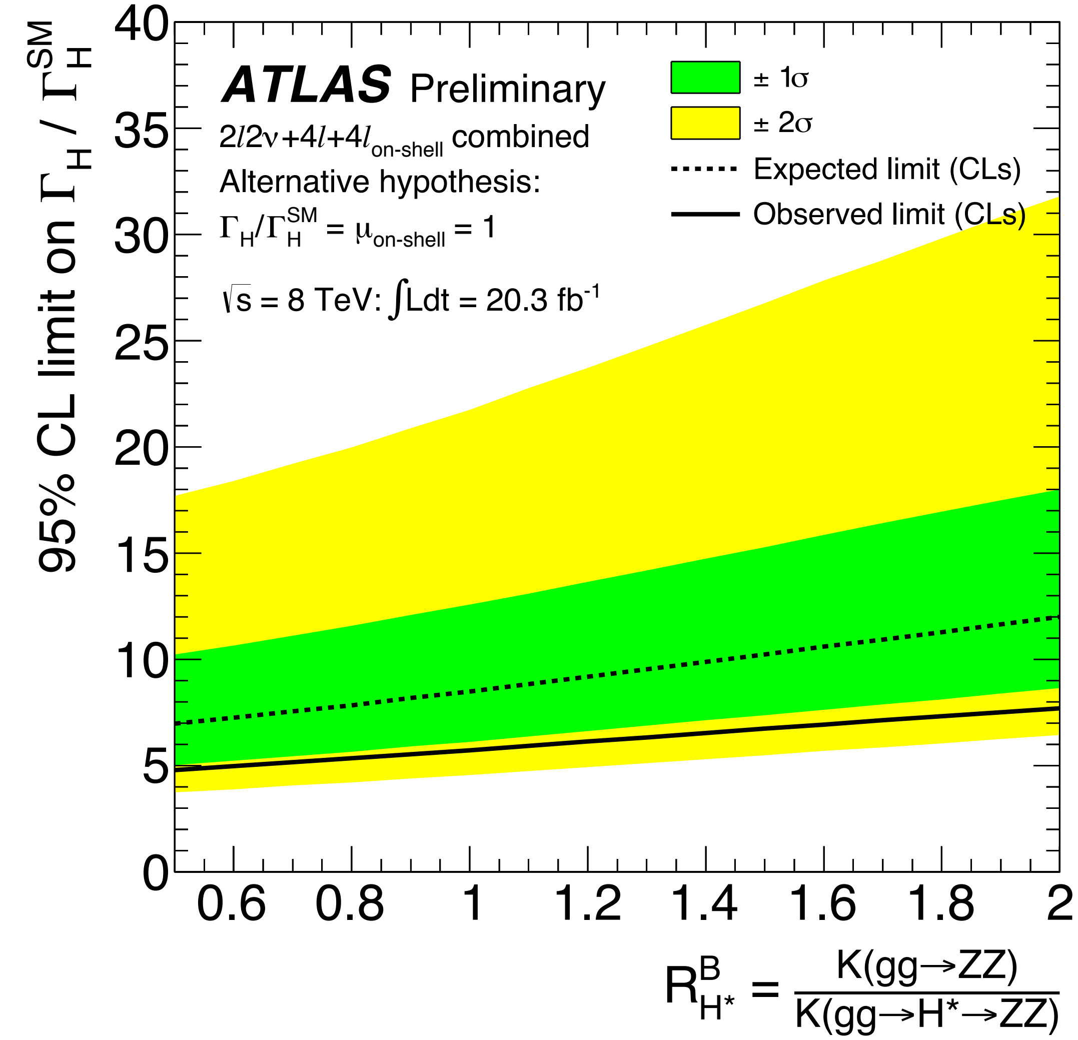

	Observed			Median expected			Alternative hypothesis
$R^B_{H^*}$	0.5	**1.0**	2.0	0.5	**1.0**	2.0	
$\mu_{\text{off-shell}}$	5.6	**6.7**	9.0	6.6	**7.9**	10.7	$R^B_{H^*} = 1, \mu_{\text{off-shell}} = 1$
Γ_H/Γ_H^{SM}	4.1	**4.8**	6.0	5.0	**5.8**	7.2	$R^B_{H^*} = 1, \Gamma_H/\Gamma_H^{SM} = 1, \mu_{\text{on-shell}} = 1.51$
Γ_H/Γ_H^{SM}	4.8	**5.7**	7.7	7.0	**8.5**	12.0	$R^B_{H^*} = 1, \Gamma_H/\Gamma_H^{SM} = 1, \mu_{\text{on-shell}} = 1$

$H \rightarrow \gamma\gamma$

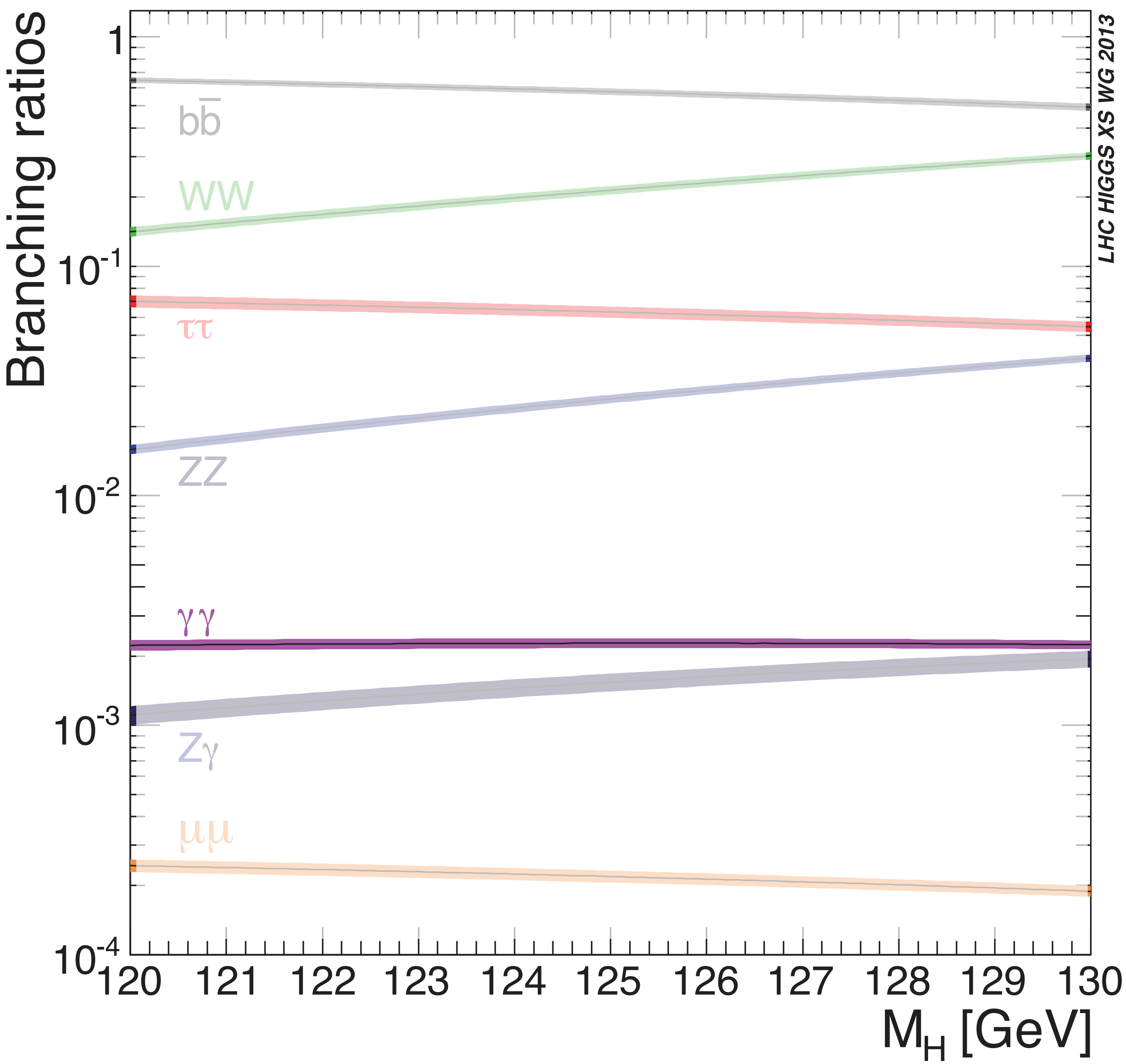

Highlights

- S/B ~ 3-4% at $m_H = 125$ GeV
- Excellent mass resolution: 1.7 GeV
- $\sigma \cdot$ BR ~ 45 fb for m_H=125.5 GeV @ 8 TeV

Latest public results

- Mass: arXiv:1406.3827 accepted by PRD
- Couplings: Phys. Lett. B726 (2013) 88 / ATLAS-CONF-2013-012
- Differential Cross-Sections: arXiv:1407.4222 submitted to JHEP
- Spin/CP: Phys. Lett. B726 (2013) 120

$H \rightarrow \gamma\gamma$: analysis

NEW

- Event selection:
  - two isolated photons, $p_T/m_{\gamma\gamma}>0.35,0.25$
    - Excellent γ ID: 75% $\gamma\gamma$ after cuts
  - photon pair vertex from tracks and calorimeter segmentation
  - 10 categories based on: (un)converted photons, detector region and p_{Tt}*
- New e/γ calibration: 10% improvement in resolution
- Main backgrounds:
  - di-photon production (~80%)
  - γj and jj (~20%)
  - modeled with analytical functions and fit in the 105-160 GeV range

$$^{*}p_{\mathrm{Tt}} = |(\boldsymbol{p}_{\mathrm{T}}^{\gamma_1} + \boldsymbol{p}_{\mathrm{T}}^{\gamma_2}) \times \hat{\mathbf{t}}|, \text{ where } \hat{\mathbf{t}} = \frac{\boldsymbol{p}_{\mathrm{T}}^{\gamma_1} - \boldsymbol{p}_{\mathrm{T}}^{\gamma_2}}{|\boldsymbol{p}_{\mathrm{T}}^{\gamma_1} - \boldsymbol{p}_{\mathrm{T}}^{\gamma_2}|}$$

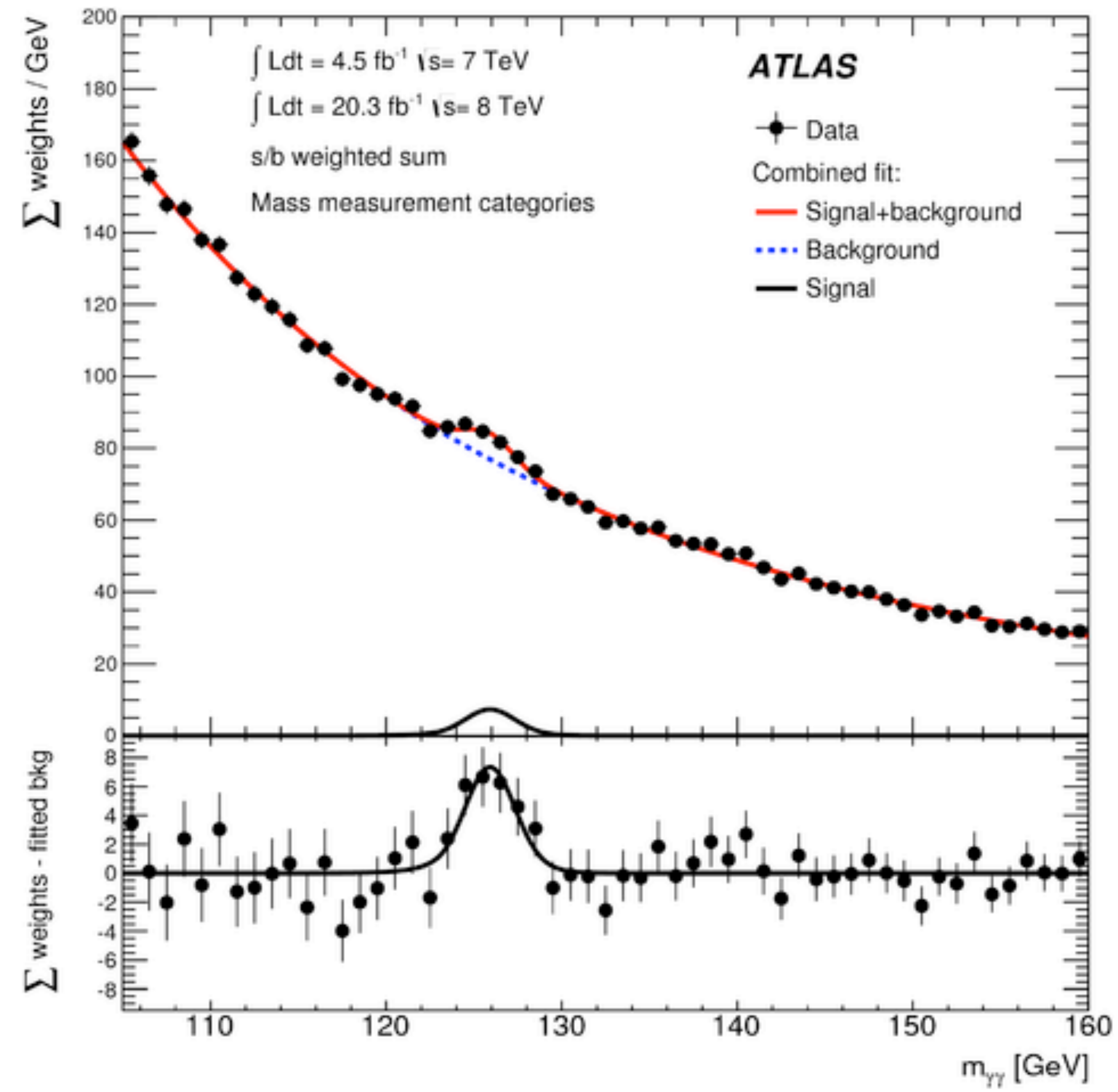

$m_H = 125.98 \pm 0.42$ (stat) ± 0.28 (syst) GeV

$\mu = 1.29 \pm 0.30$ (at $m_H = 125.98$)

$H\rightarrow\gamma\gamma$: fiducial cross section

NEW

- Measurement of inclusive fiducial cross sections:
  - Baseline: two isolated photons with $p_T/m_{\gamma\gamma} > 0.35, 0.25$ and with $|\eta| < 2.37$

$\sigma_{meas} = 43.2 \pm 9.4\,(\text{stat})\,^{+3.2}_{-2.9}\,(\text{syst}) \pm 1.2(\text{lumi})$, @$m_H$=125.4 GeV

$\sigma_{theory} = 30.5 \pm 3.3$

  - Jet multiplicity, VBF enhanced, *lepton multiplicity and *high E_T^{miss} (*upper limits)
- Measurement of differential cross sections in the baseline fiducial volume:
  - Higgs boson kinematics, jet activity, spin-CP sensitive variables, VBF-sensitive variables
- Overall agreement in shape between data and Standard Model expectations

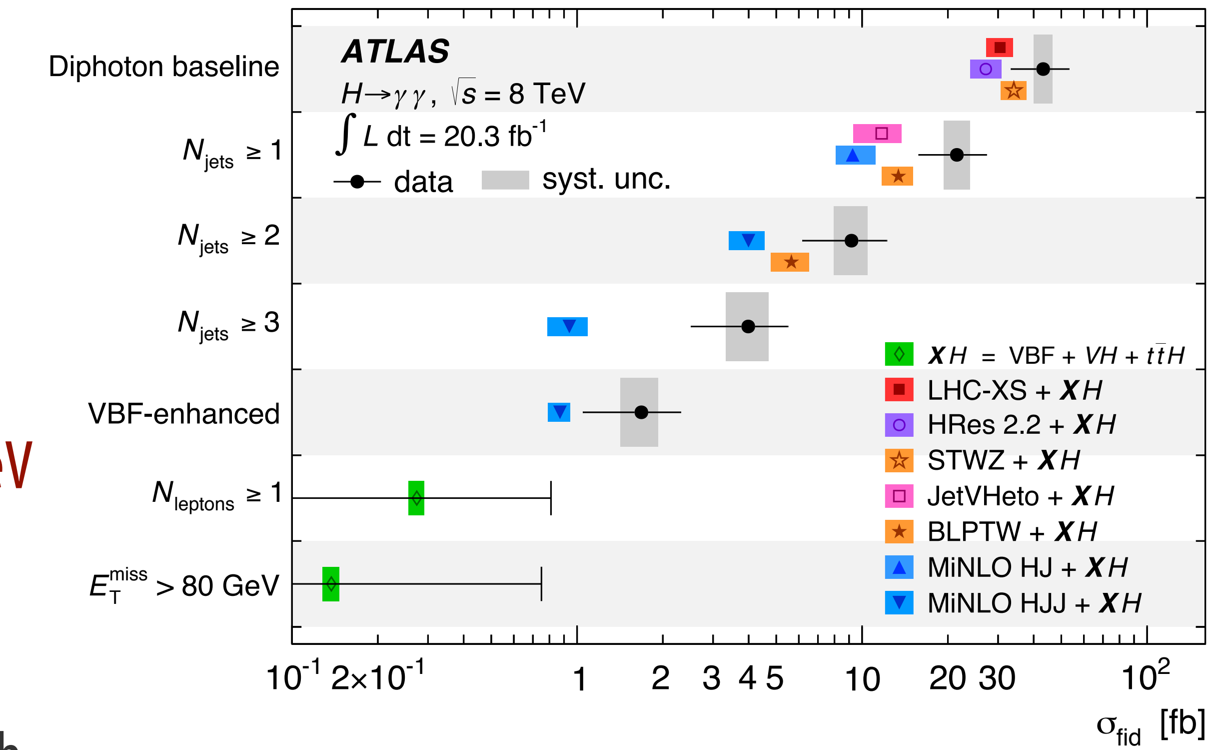

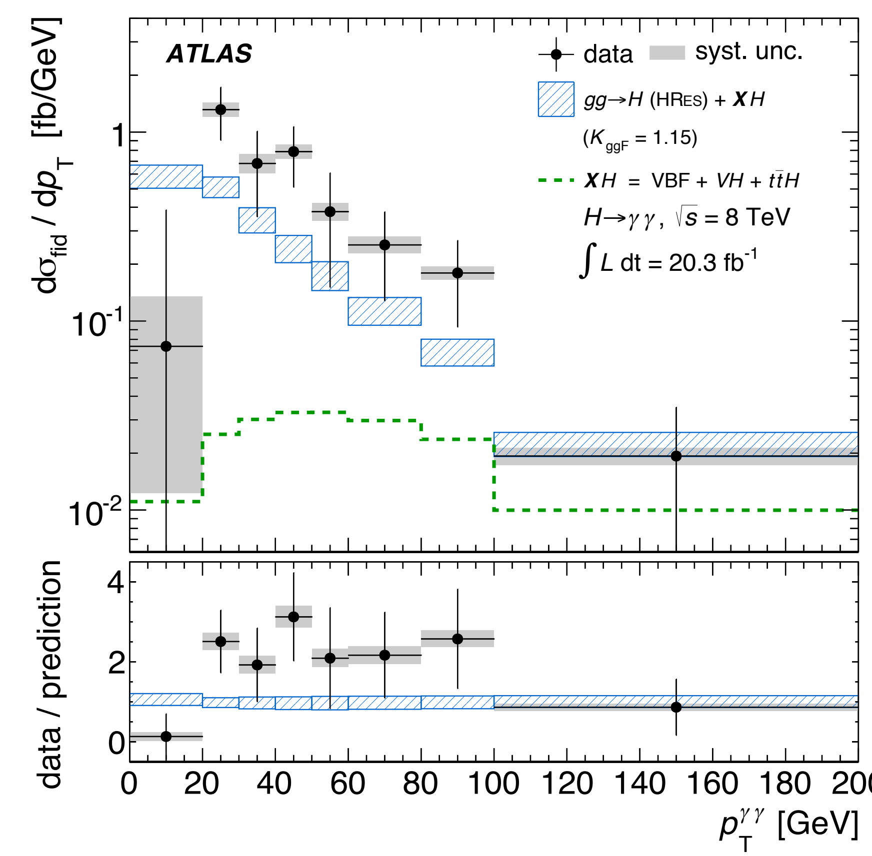

$H \to \gamma\gamma + H \to ZZ \to 4\ell$ combination

NEW

- New mass measurement just made public
- Total uncertainty reduced by ~40%
  - Systematics reduced by factor ~3
- Compatibility between channels:
  - 1.97σ (was 2.5σ)
    - 1.6σ if fixing both signal strengths to 1
    - 1.8σ if using "box-like" systematics for γ energy scale

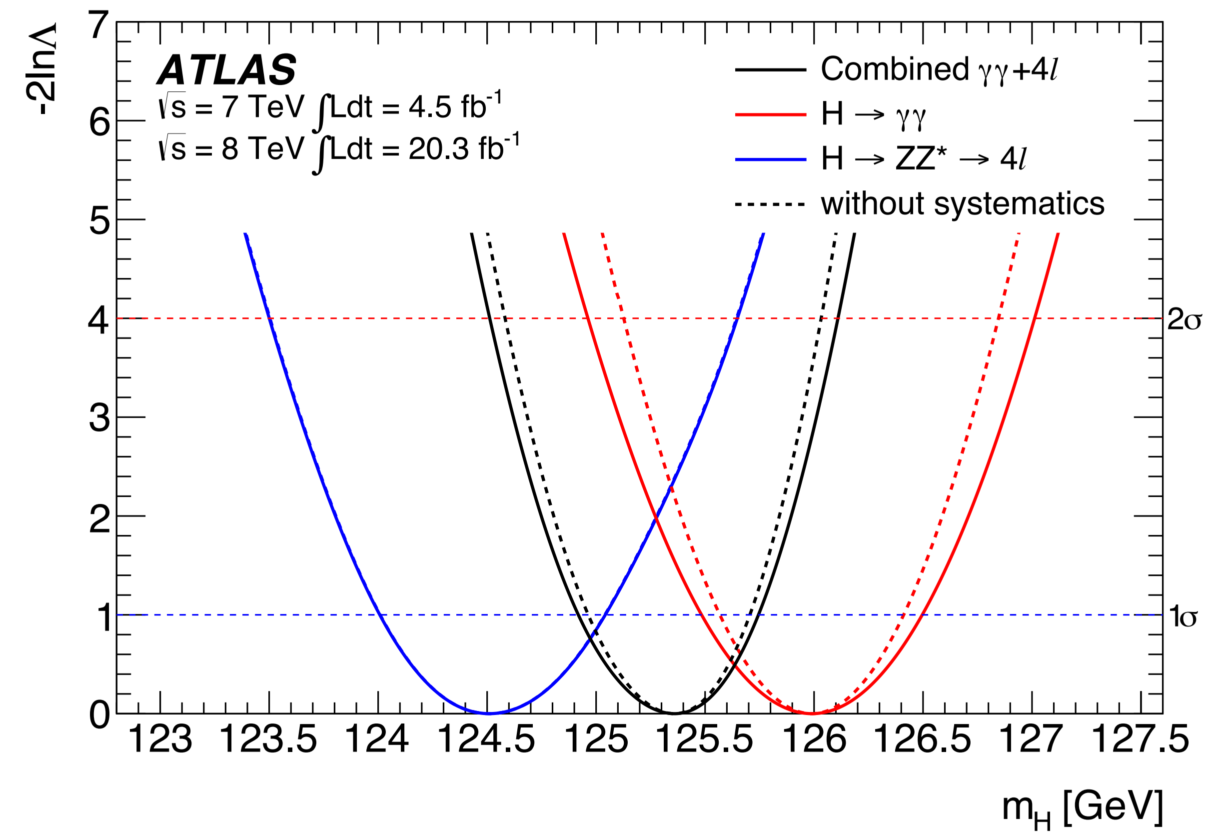

Channel	Mass measurement [GeV]
$H \to \gamma\gamma$	$125.98 \pm 0.42\,(\text{stat}) \pm 0.28\,(\text{syst}) = 125.98 \pm 0.50$
$H \to ZZ^* \to 4\ell$	$124.51 \pm 0.52\,(\text{stat}) \pm 0.06\,(\text{syst}) = 124.51 \pm 0.52$
Combined	$125.36 \pm 0.37\,(\text{stat}) \pm 0.18\,(\text{syst}) = 125.36 \pm 0.41$

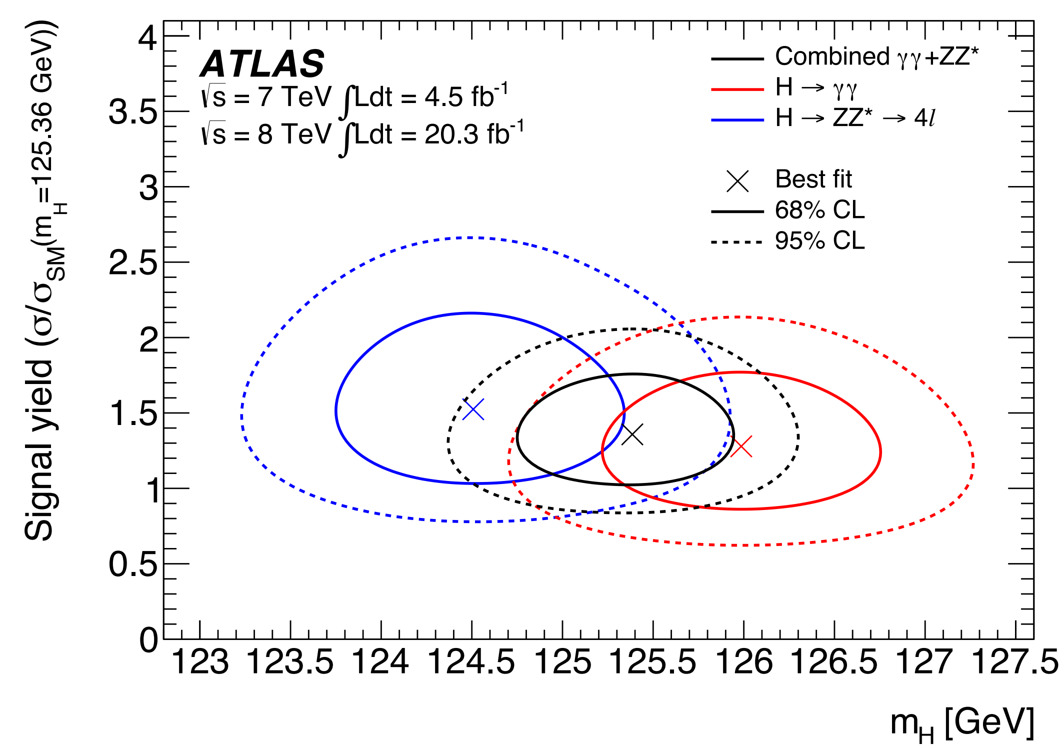

More on O. Kortner's talk

$H \rightarrow WW \rightarrow \ell\ell\nu\nu$

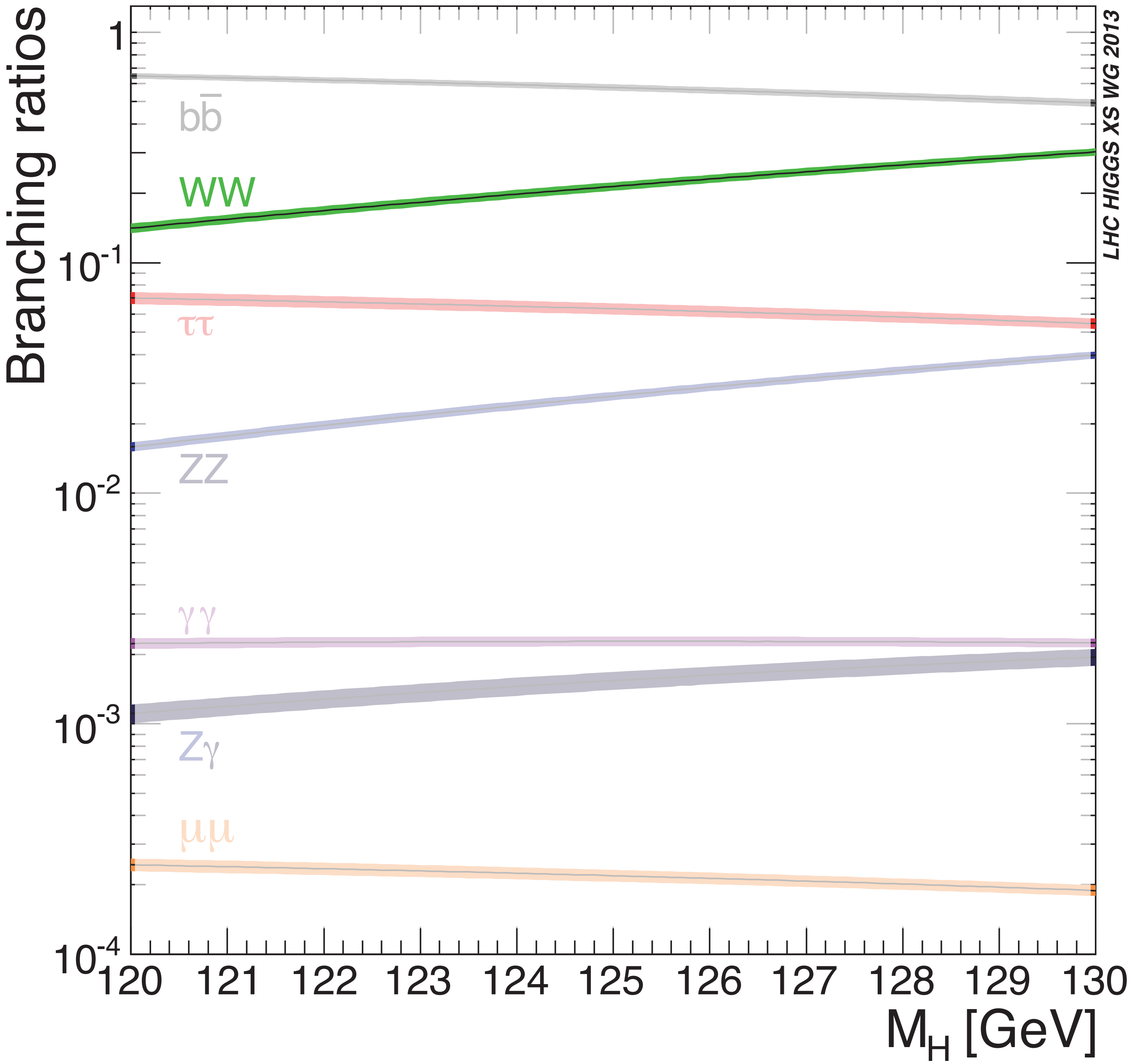

Highlights

- S/B ~ 0.3 in most sensitive category
- No reconstructed mass peak
- $\sigma \cdot BR \sim 100$ fb
  for m_H=125.5 GeV @ 8 TeV

Latest public results

- Couplings: Phys. Lett. B726 (2013) 88 -119 / ATLAS-CONF-2013-030
- Spin/CP: Phys. Lett. B726 (2013) 120-144 / ATLAS-CONF-2013-031
- VH($\rightarrow$WW): ATLAS-CONF-2013-075

H→WW→$\ell\ell\nu\nu$: analysis

- Signature: $\ell^+\ell^-$ + E_T^{miss}, no mass peak: observable m_T

$$m_T^2 = \left(\sqrt{m_{\ell\ell}^2 + |\vec{p}_{T_{\ell\ell}}|^2} + E_T^{miss}\right)^2 - \left(\vec{p}_{T_{\ell\ell}} + \vec{E}_T^{miss}\right)^2$$

- Large backgrounds: WW, W+jets, top, Z/γ*
- Local significance (at m_H=125 GeV): 3.8σ observed, 3.7σ expected
- Measured signal strength (at m_H=125 GeV): 1.01 ± 0.31

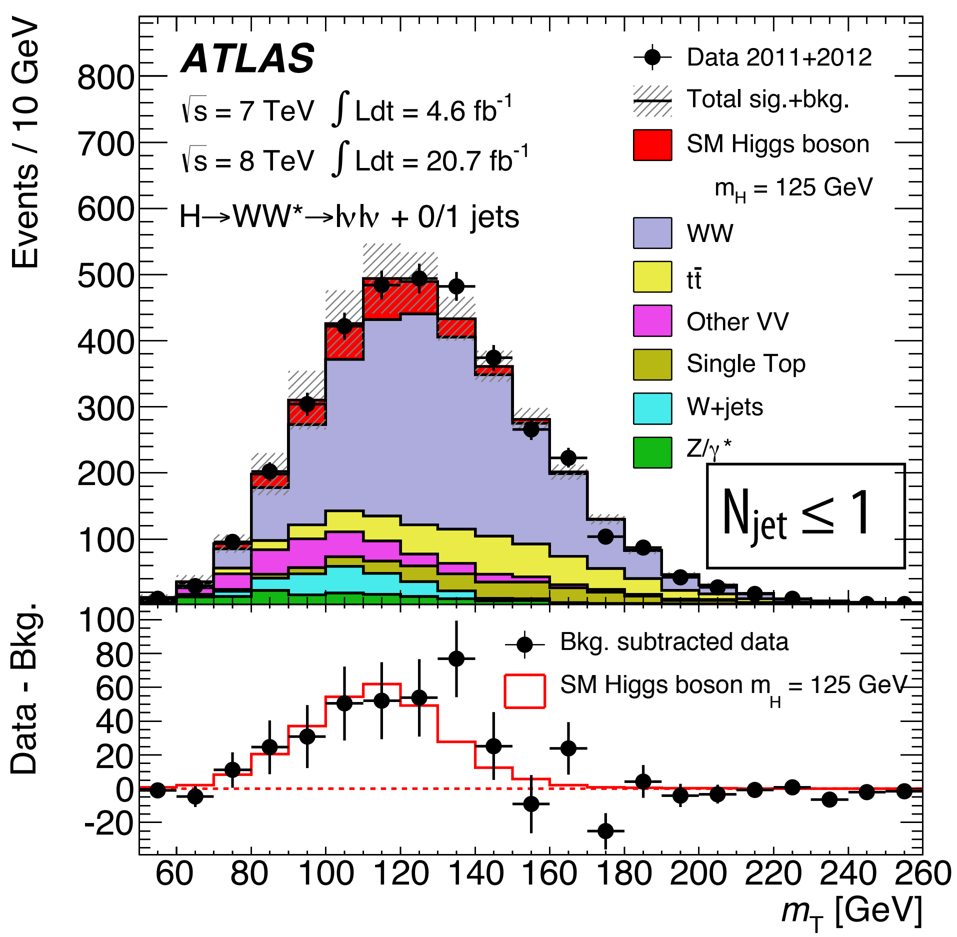

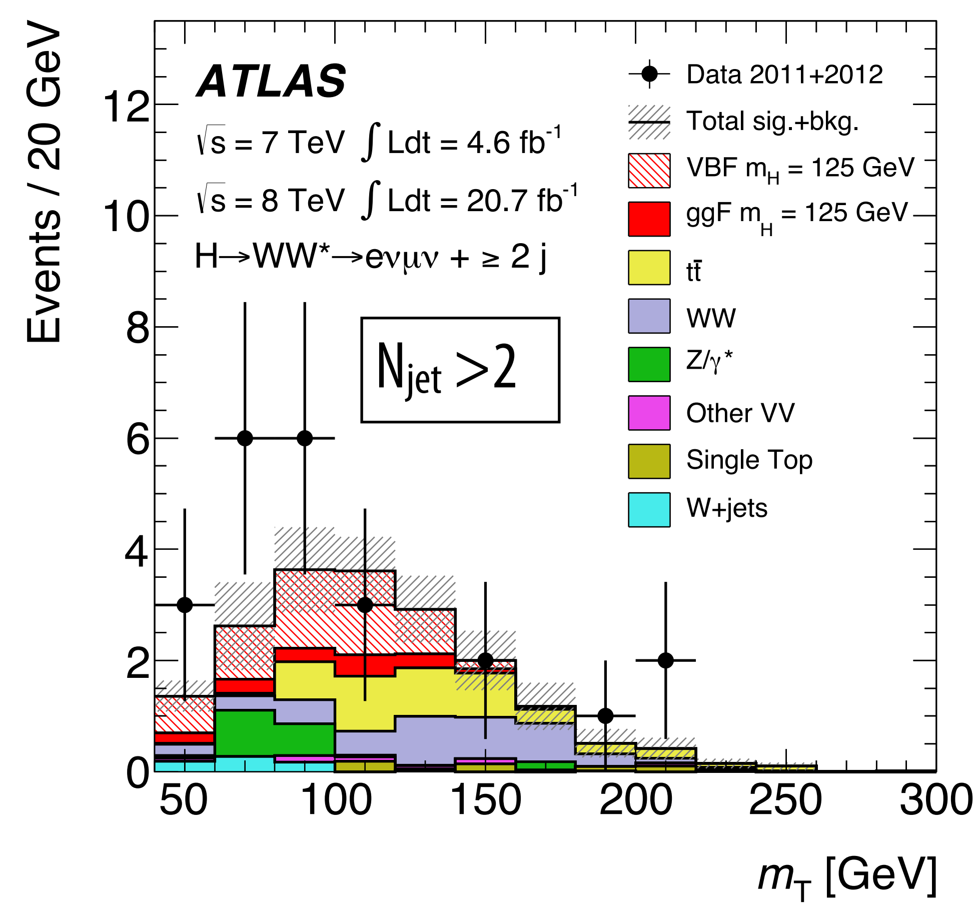

Combined Spin/CP results

- Compared Standard Model spin-parity $J^P=0^+$ hypothesis to alternative hypotheses (0^-, 1^+, 1^-, 2^+)
- All hypotheses are excluded at confidence levels above 97%
  - Independent on assumptions on the couplings to SM particles
  - Independent on the fraction of gluon-gluon or quark-antiquark production (for $J^P=2^+$)

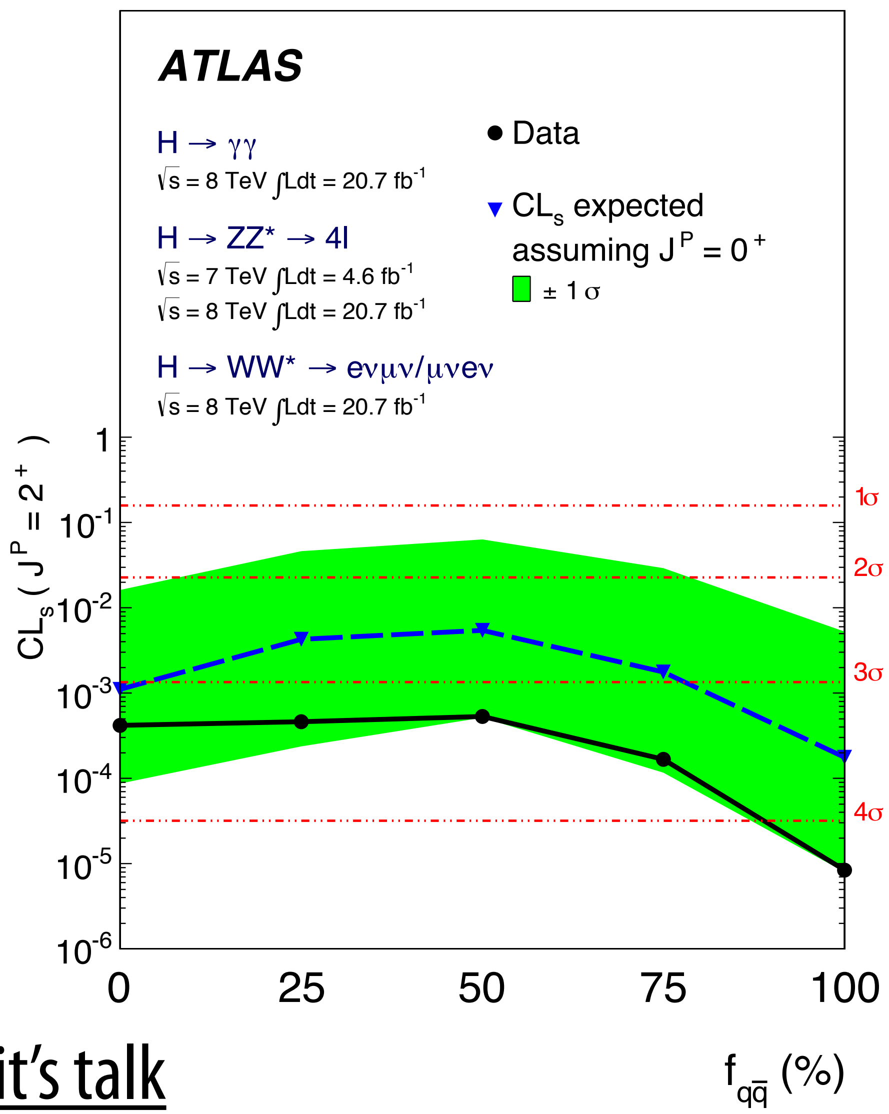

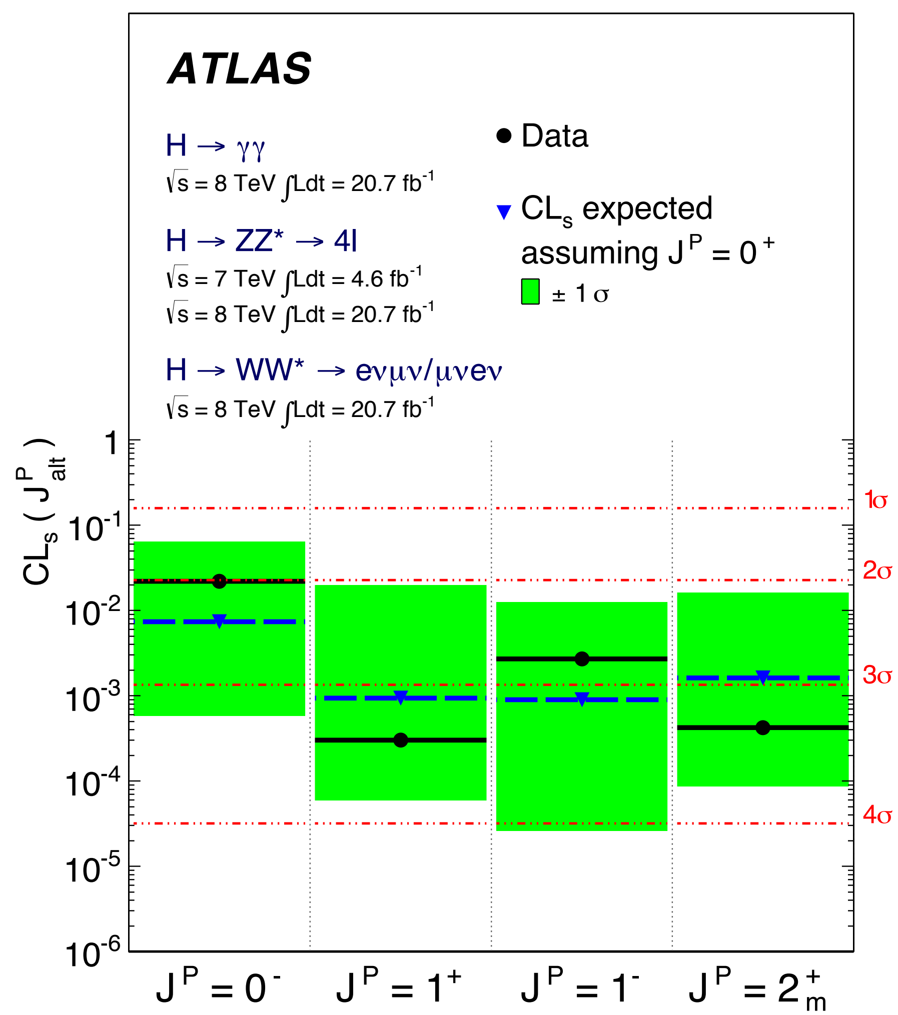

More on P. Kluit's talk

$H \to Z\gamma \to \ell\ell\gamma$

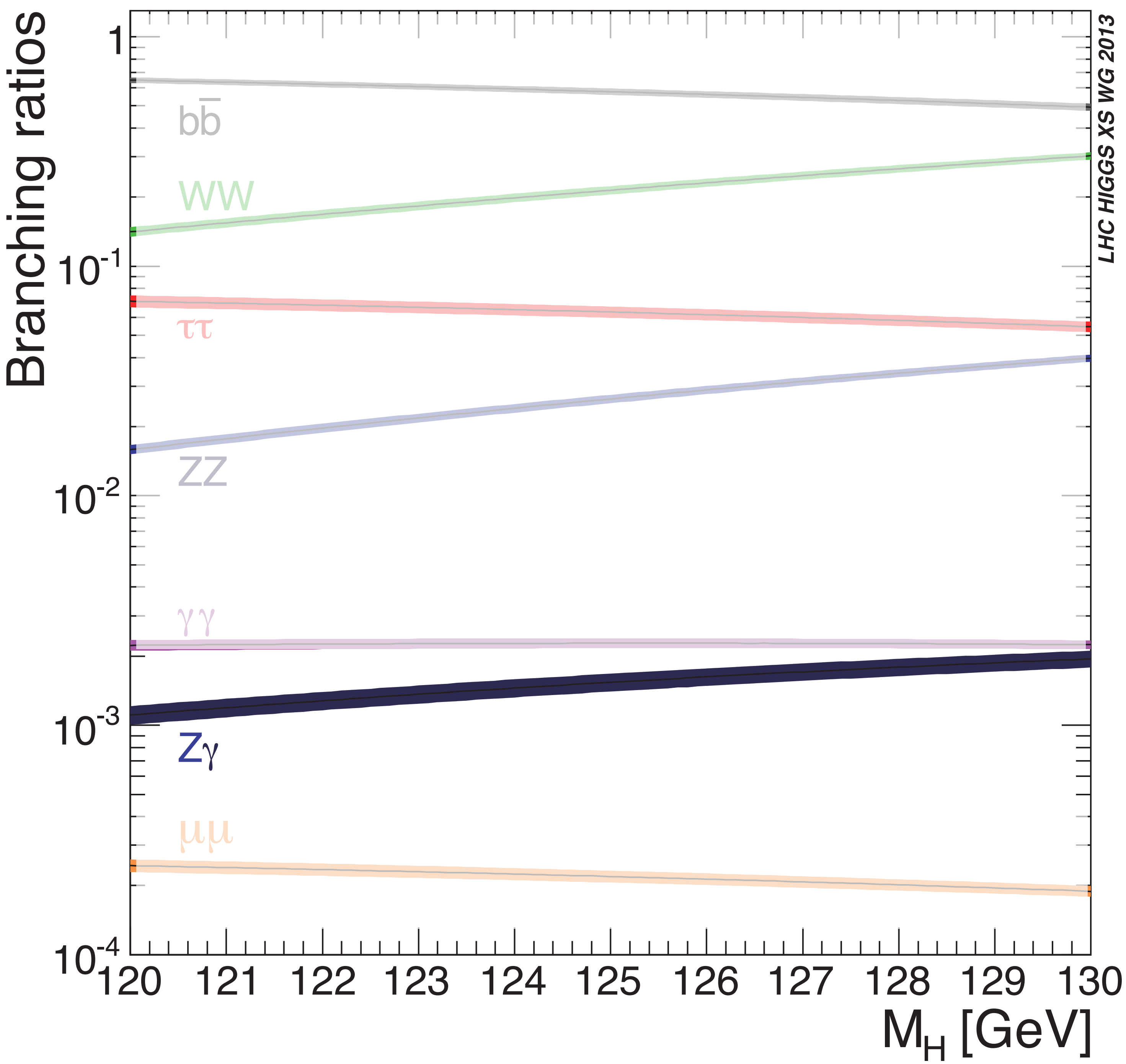

Highlights

- $\sigma \cdot \mathrm{BR} \sim 2.3$ fb
  for m_H=125.5 GeV @ 8 TeV
- S/B ranging from 0.001 to 0.01
- $\sigma(m_{\mu\mu\gamma}) = 1.6$ GeV
- Sensitive to new physics

Latest public results

- Search: Phys. Lett. B 732C (2014), pp. 8-27

H→Zγ→ℓℓγ

- Event selection: opposite-sign lepton pair (e/μ) + isolated photon with $E_T > 15$ GeV
- Backgrounds: Z + γ (82%), Z + jets (17%), ttbar (1%): modeled using analytical functions
- Categories
  - ee/μμ final states, 7/8 TeV, $\Delta\eta_{\gamma Z}$, p_{Tt}
- 95% CL limit at $m_H = 125.5$ GeV: obs 11(exp 9) x SM

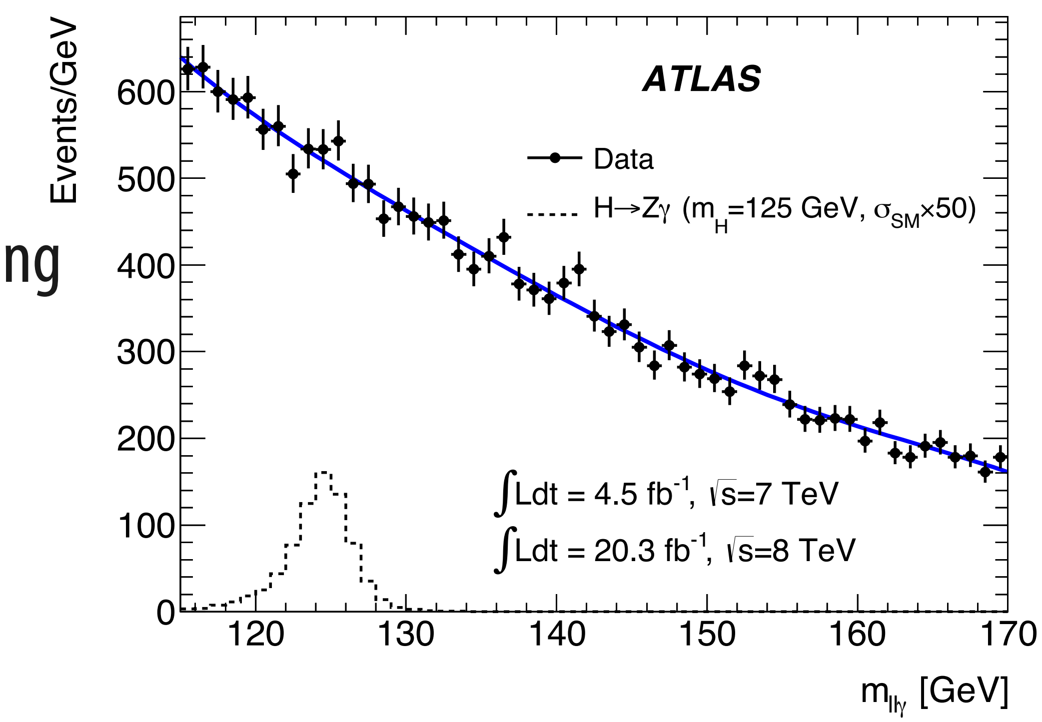

$\sqrt{s}$ [TeV]	ℓ	Category	N_S	N_B	N_D	$\frac{N_S}{\sqrt{N_B}}$	FWHM [GeV]
8	μ	high p_{Tt}	2.3	310	324	0.13	3.8
8	μ	low p_{Tt}, low $\Delta\eta$	3.7	1600	1587	0.09	3.8
8	μ	low p_{Tt}, high $\Delta\eta$	0.8	600	602	0.03	4.1
8	e	high p_{Tt}	1.9	260	270	0.12	3.9
8	e	low p_{Tt}, low $\Delta\eta$	2.9	1300	1304	0.08	4.2
8	e	low p_{Tt}, high $\Delta\eta$	0.6	430	421	0.03	4.5
7	μ	high p_{Tt}	0.4	40	40	0.06	3.9
7	μ	low p_{Tt}	0.6	340	335	0.03	3.9
7	e	high p_{Tt}	0.3	25	21	0.06	3.9
7	e	low p_{Tt}	0.5	240	234	0.03	4.0

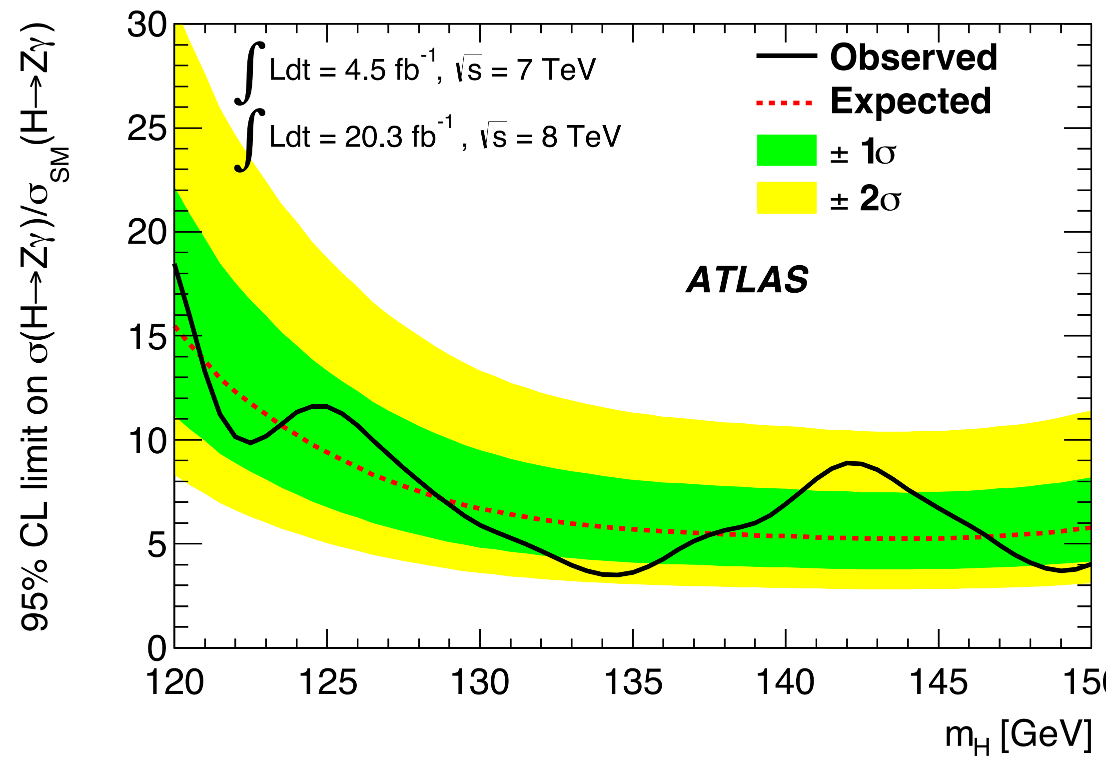

Summary

- Many new/updated measurements this summer for Higgs decaying into bosonic final states!
    - More to come in the near future
- Presented latest results by ATLAS in this sector :
    - Combined mass measurement using $H \rightarrow ZZ \rightarrow 4l$ and $H \rightarrow \gamma\gamma$: **125.36 ± 0.37 (stat) ± 0.18 (syst)**
    - Production rates, inclusive and categorized: all compatible with Standard Model expected values
    - Indirect measurement of Γ_H via high-mass $H \rightarrow ZZ$
    - Evidence for the spin-0 nature of the Higgs boson
    - Search for rare decay of $H \rightarrow Z\gamma$
    - First differential cross sections in $H \rightarrow ZZ \rightarrow 4l$ and $H \rightarrow \gamma\gamma$

Backup Slides

New electron calibration

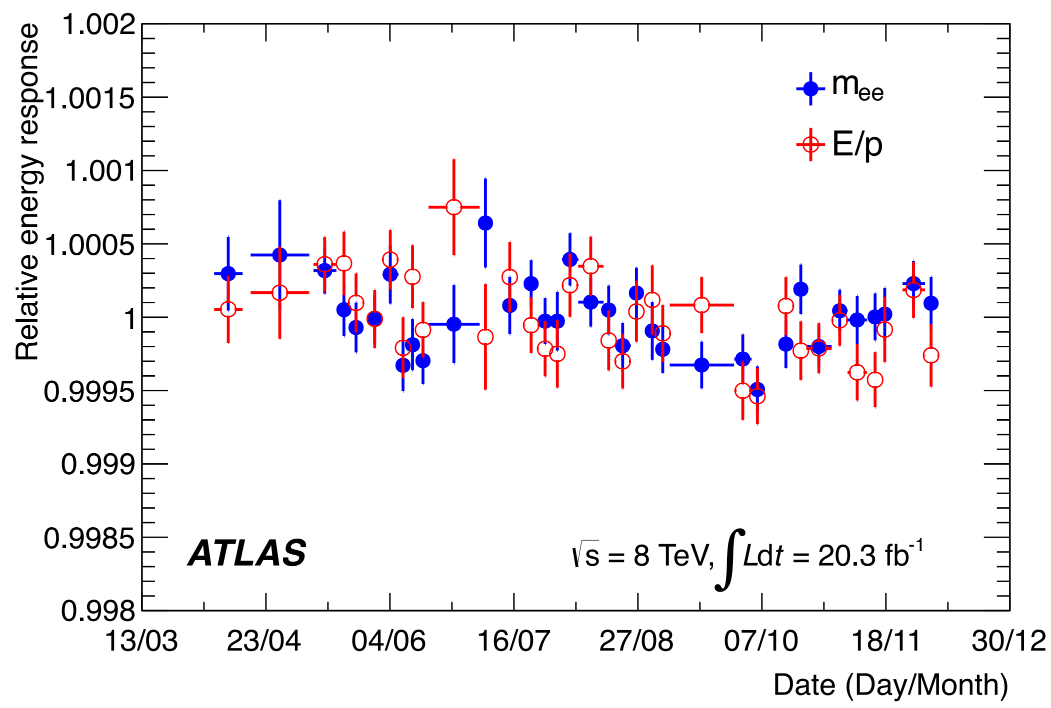

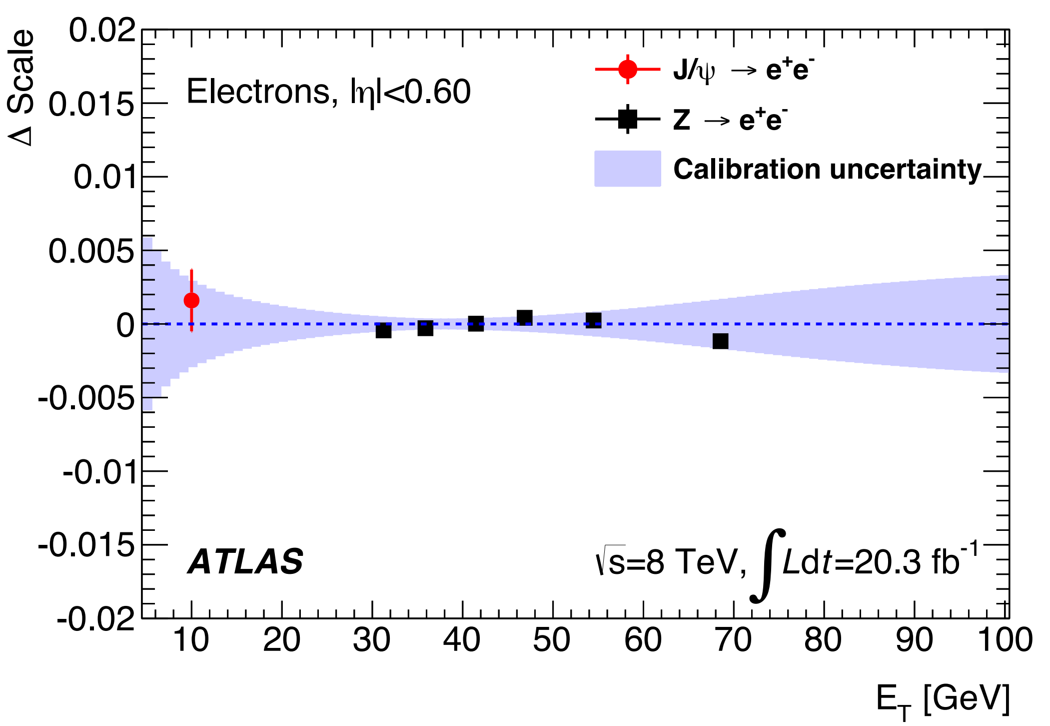

- Intercalibration of calorimeter layers using $Z \to \mu\mu$ events
  - 1-2% for EM layers 1 & 2
- Accurate knowledge of material in front of EM calorimeter
  - Constrain inactive material (2-5 X_0) to ~2-10% X_0
- EM cluster energy correction via MVA regression
- Energy scale and resolution extracted with $Z \to ee$ and $J/\psi \to ee$
  - Good data/MC agreement after corrections
- Response stable at ~0.05% vs time and pileup

Leptons improvements

- New electron likelihood-based identification selection
  - same signal efficiency as cut-based
  - improves rejection of light-flavor jets and photon conversions by a factor ~2
- New electron combined fit of the track momentum and cluster energy
  - for $E_T < 30$ GeV and when track momentum and cluster energy are consistent
  - improves m4ℓ resolution in 4e and 2μ2e channels by ~4%
- Improved muon momentum scale and resolution corrections
  - determined using $Z \rightarrow \mu\mu$ and $J/\psi \rightarrow \mu\mu$, checked with $\Upsilon \rightarrow \mu\mu$
  - momentum scale uncertainties: 0.05% in barrel, up to 0.2% for $|\eta| > 2$

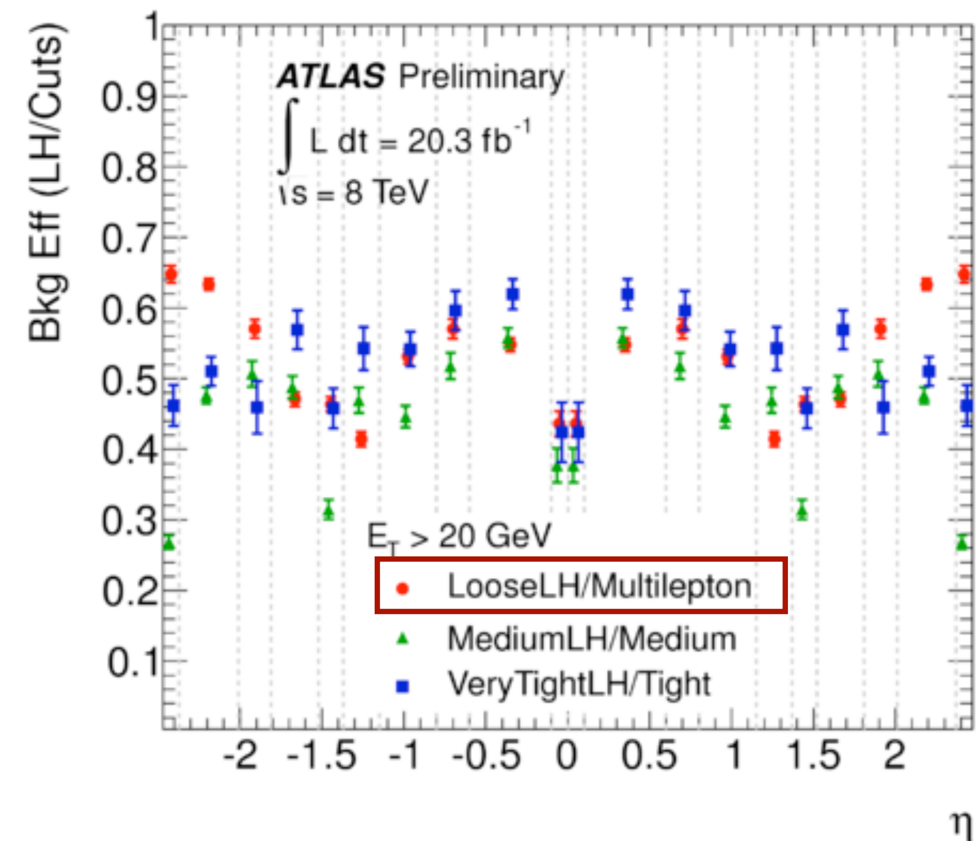

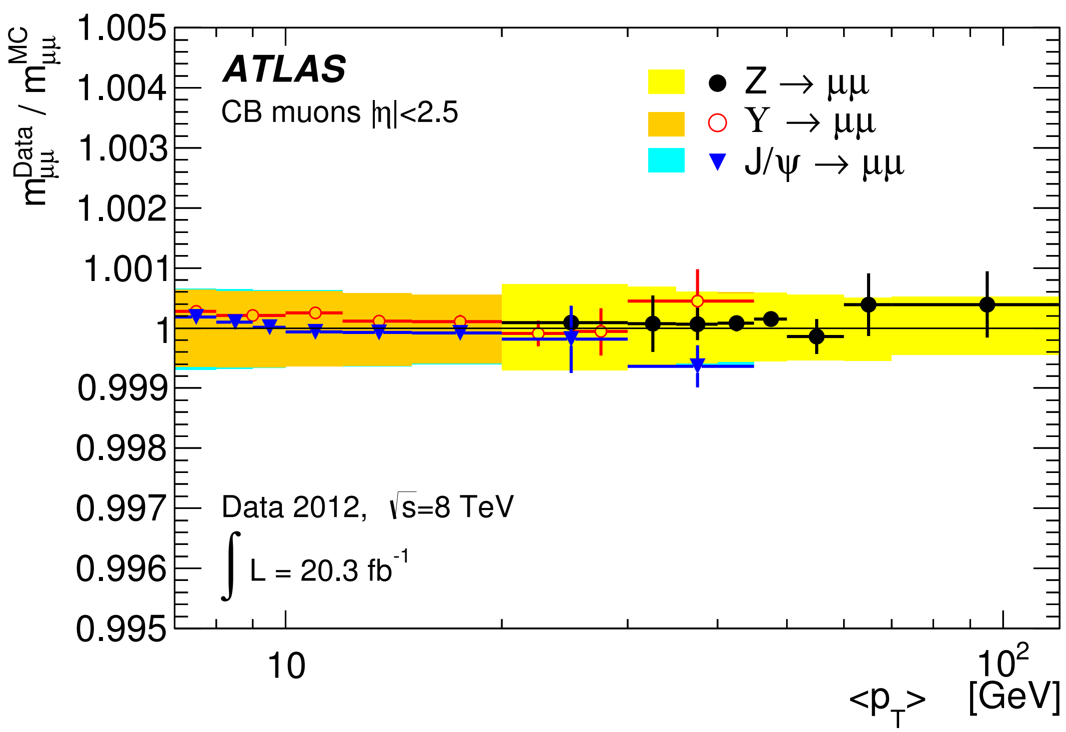

Split decay modes

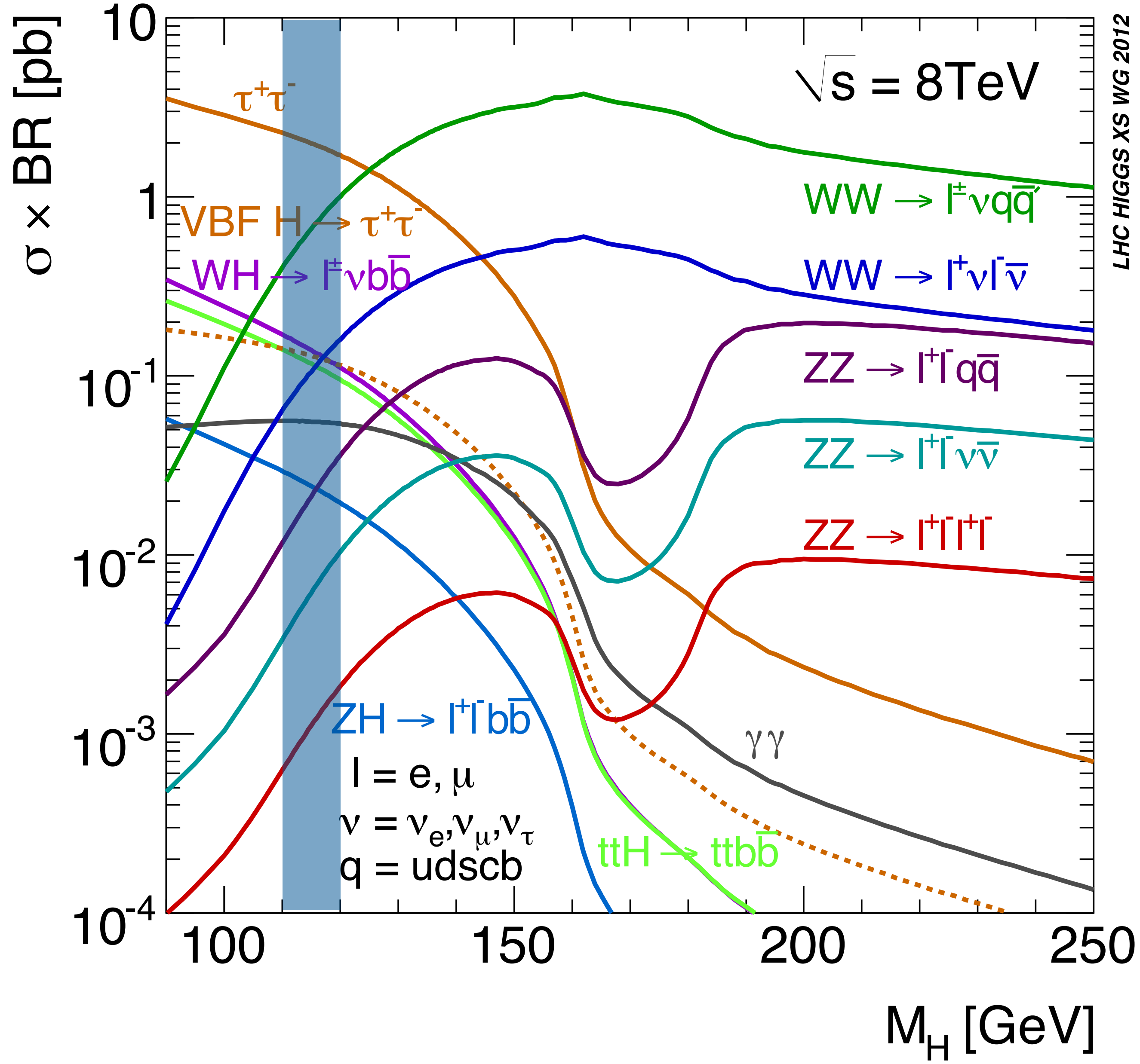

H→ZZ→4ℓ: Event Selection (1)

- Electrons:
  - E_T>7 GeV, |η|<2.47
  - improved reconstruction algorithm with higher efficiency in 2012
  - likelihood-based selection (cut-based for 7 TeV)
- Muons:
  - p_T>6 GeV, |η|<2.7
- Quality and cleaning cuts; e-e, e-μ, e-jet overlap removal
- Quadruplets: 2 SF OS lepton pairs
  - p_{T1}>20 GeV, p_{T2}>15 GeV, p_{T3}>10 GeV
- Single- and dilepton trigger object(s) matched to the lepton(s)

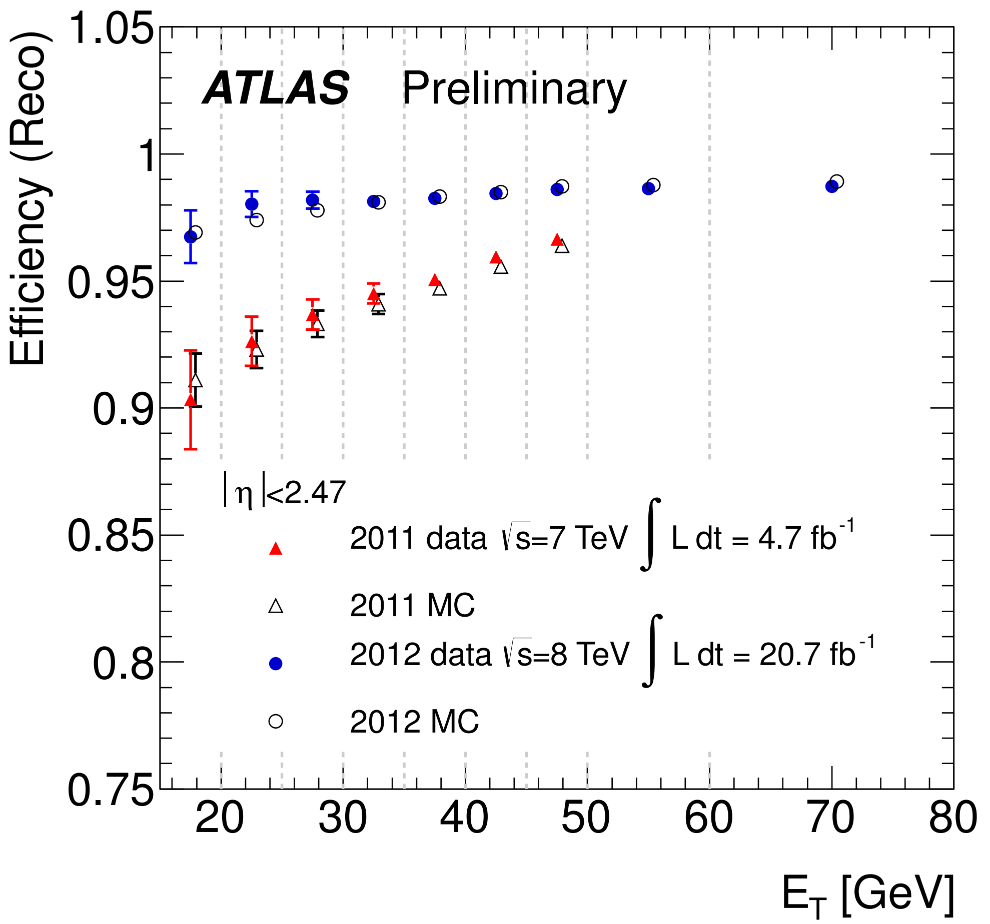

$H\rightarrow ZZ\rightarrow 4\ell$: Event Selection (2)

- Select lepton pair with the mass closest to the Z boson mass : Z_1
  - Leading pair: $50 < m_{12} < 106$ GeV
- Among remaining pairs, select the next-closest to m_Z : Z_2
  - Subleading pair: $m_{min} < m_{34} < 115$ GeV, $m_{min} = 12$ (50) for m4l≤140 (≥190) GeV
- ΔR>0.1 (0.2) between same (opposite) flavour leptons
- Relative track isolation in cone ΔR=0.2: $I_{track} < 0.15$
- Relative calorimeter isolation in cone ΔR=0.2: typically $I_{calo} < 0.3$
- $|d_0/\sigma(d_0)| < 3.5$ (6.5) for muons (electrons)
- FSR recovery
  - collinear FSR for leading dimuon pairs (~4% of events)
  - far FSR with high E_T for leading dimuon and dielectrons (~1% of events)

Overall accepance
for m_H =125 GeV @ 8 TeV:
39% 4μ, 27% 2e2μ and 20% 4e

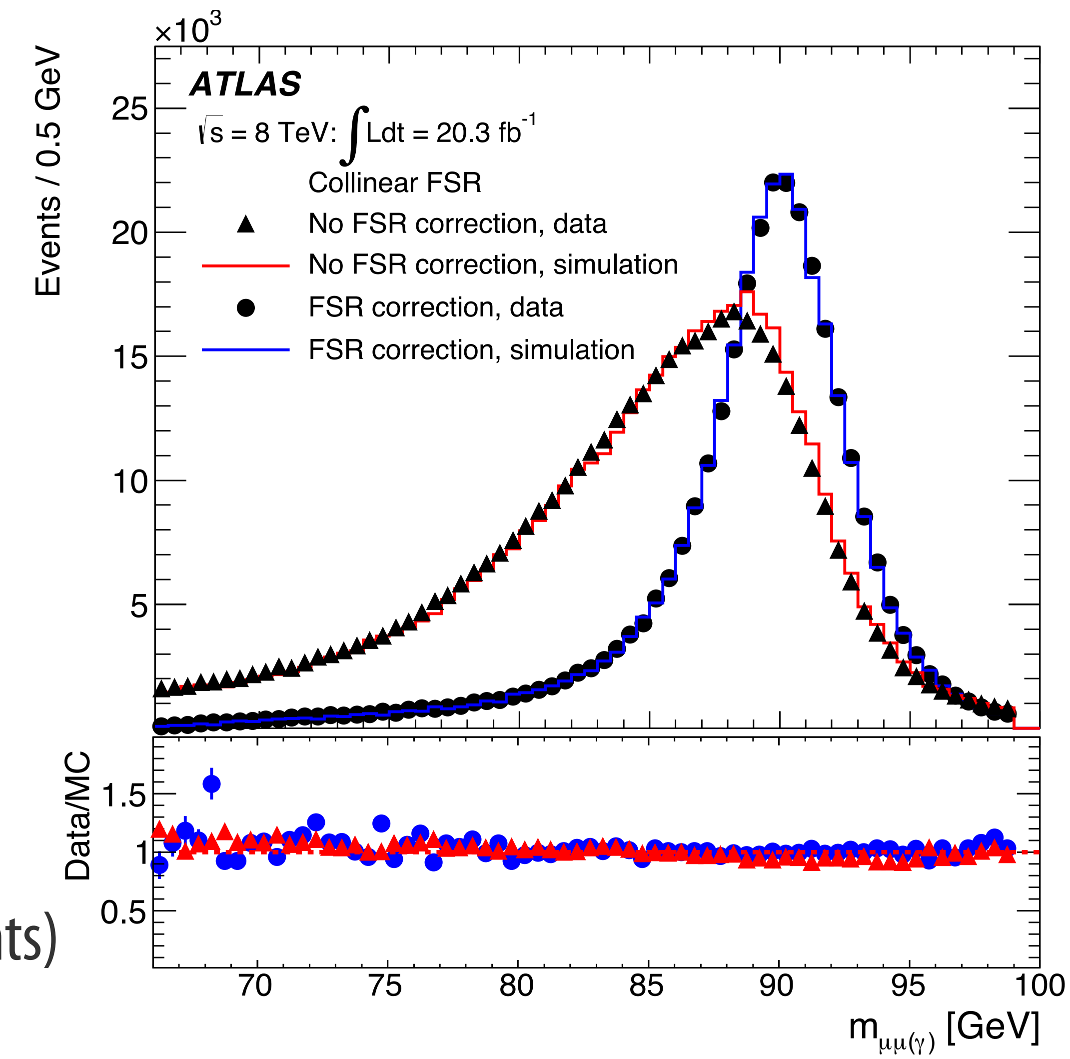

$H \rightarrow ZZ \rightarrow 4\ell$: Backgrounds (1)

Events in 120-130 GeV:
7.41 ± 0.40

- Irreducible background: ZZ*
  - main source of background
  - estimated from MC (POWHEG+gg2ZZ+SHERPA)
  - normalized to MCFM cross-section

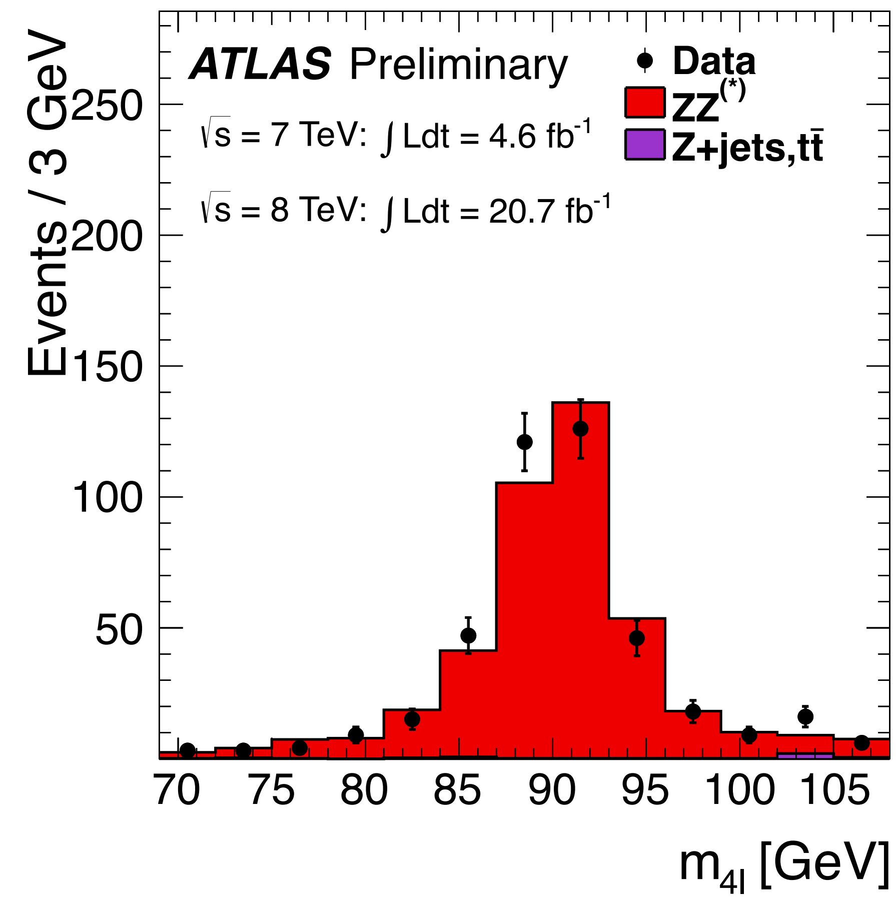

- To reduce impact of the ZZ*background on the fitted mass use BDT discriminant
  - p_T of four lepton system
  - η of four lepton system
  - matrix element based kinematic discriminant

$$D_{ZZ^*} = \ln\left(\frac{|M_{sig}|^2}{|M_{ZZ}|^2}\right)$$

H→ZZ→4ℓ: Backgrounds (2)

- Reducible backgrounds: Z+jets (including Z+bb) and tt
  - estimated separately for final states with subleading muons and electrons
  - data-driven methods
- *ℓℓ+μμ* channels
  - Four CRs are fitted simultaneously to extract each component of the reducible background
  - Fitted yields extrapolated to signal region using efficiencies from simulation
  - Small contribution from WZ decays estimated using simulation
- *ℓℓ+ee* channels
  - 3*ℓ*+*X* CR - full selection on 3*ℓ*, relaxed ID on X, SS
  - fit to hits in B-layer and TRT threshold
  - fitted yields extrapolated to the signal region using efficiencies from Z+X

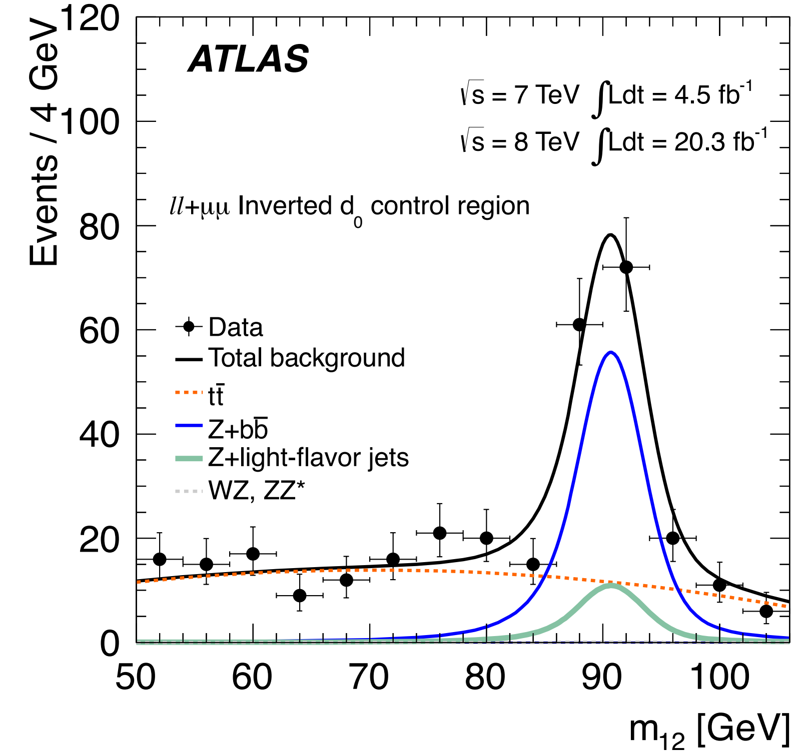

Total estimate in 120-130 GeV: 2.95 ± 0.33

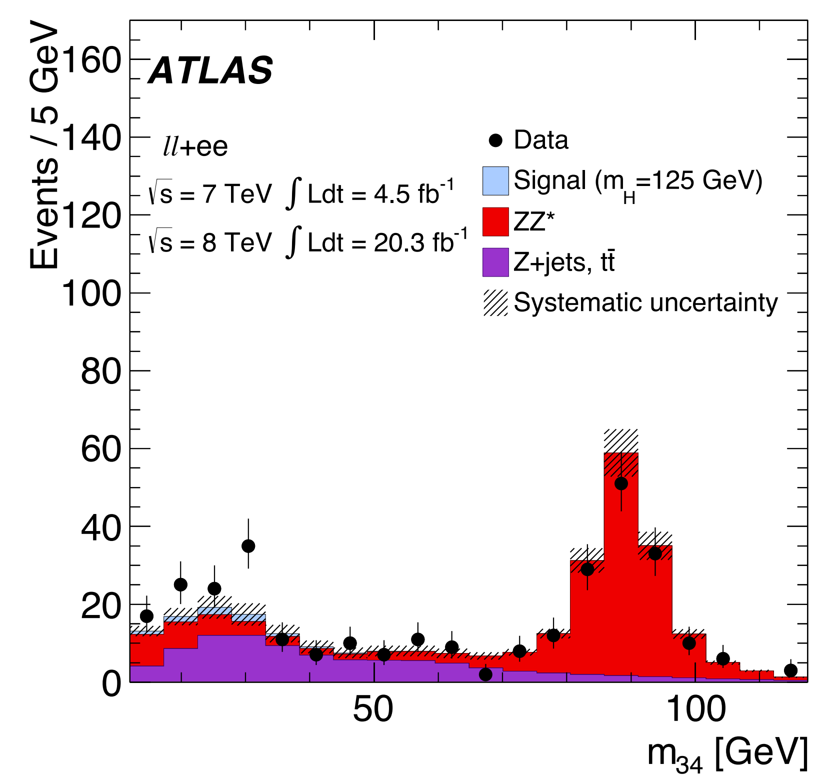

$H \rightarrow ZZ \rightarrow 4\ell$: Mass measurement (1)

- Kinematic fit used to constrain m_{Z1} to the Z pole mass within the experimental resolution
  - improvement on the $m_{4\ell}$ resolution of ~15%
- Two-dimensional fit to $m_{4\ell}$ and BDT_{ZZ^*}
  - ~8% improvement over simple $m_{4\ell}$ fit
- Signal model based on smoothed simulation distributions
  - templates parameterized as a function of m_H
- 26.5 events expected, 37 observed

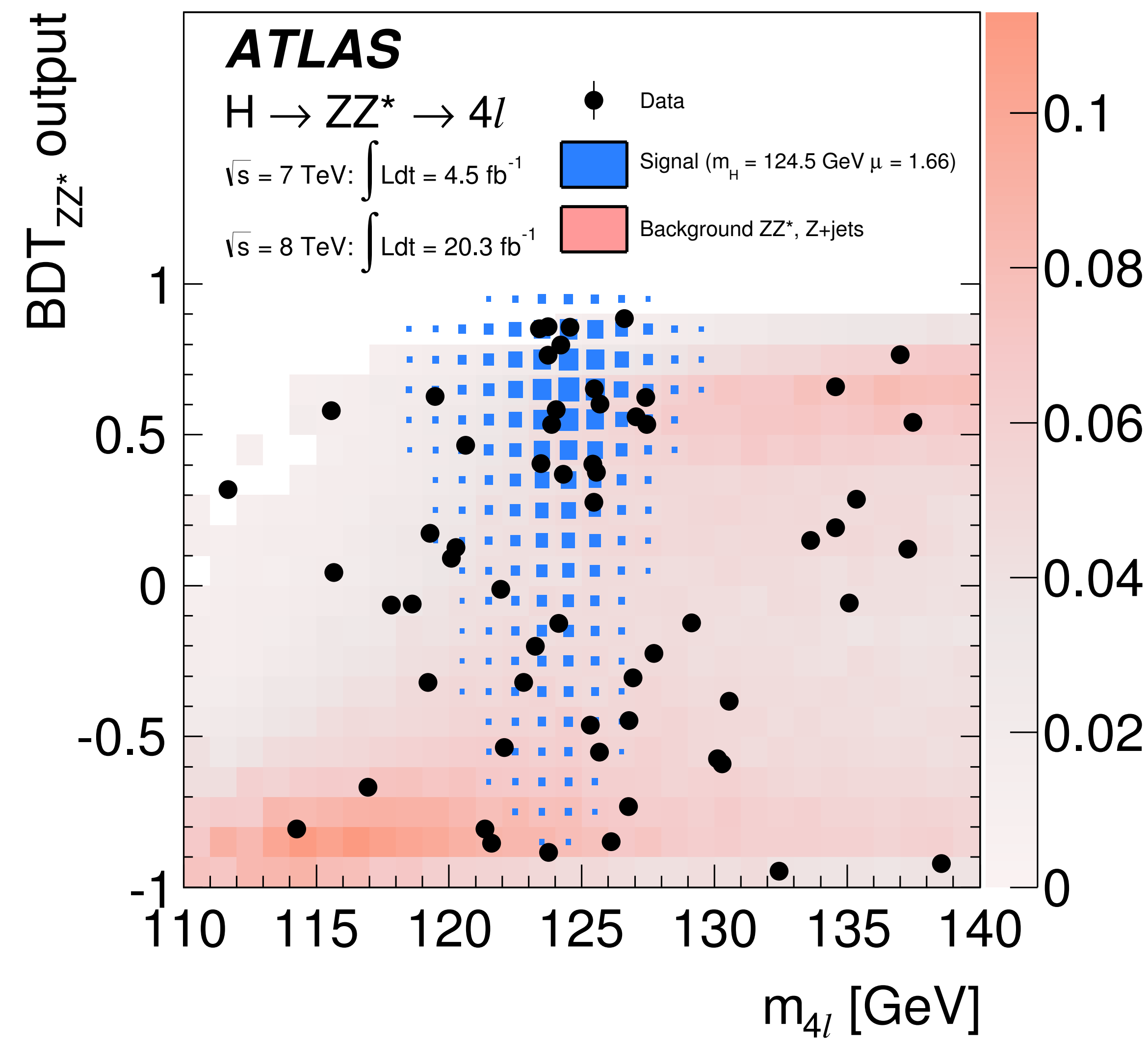

H→ZZ→4ℓ: Mass measurement (2)

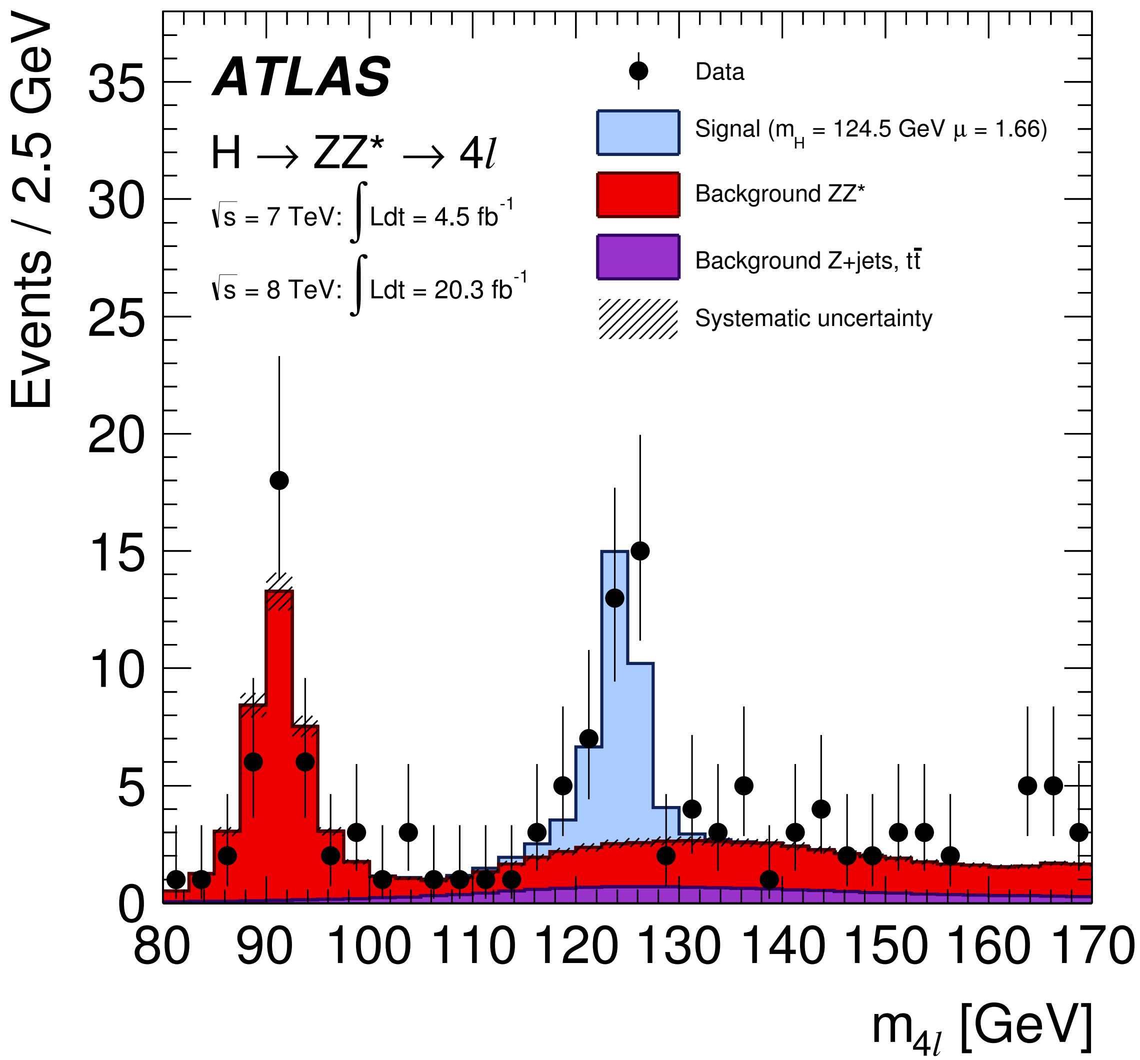

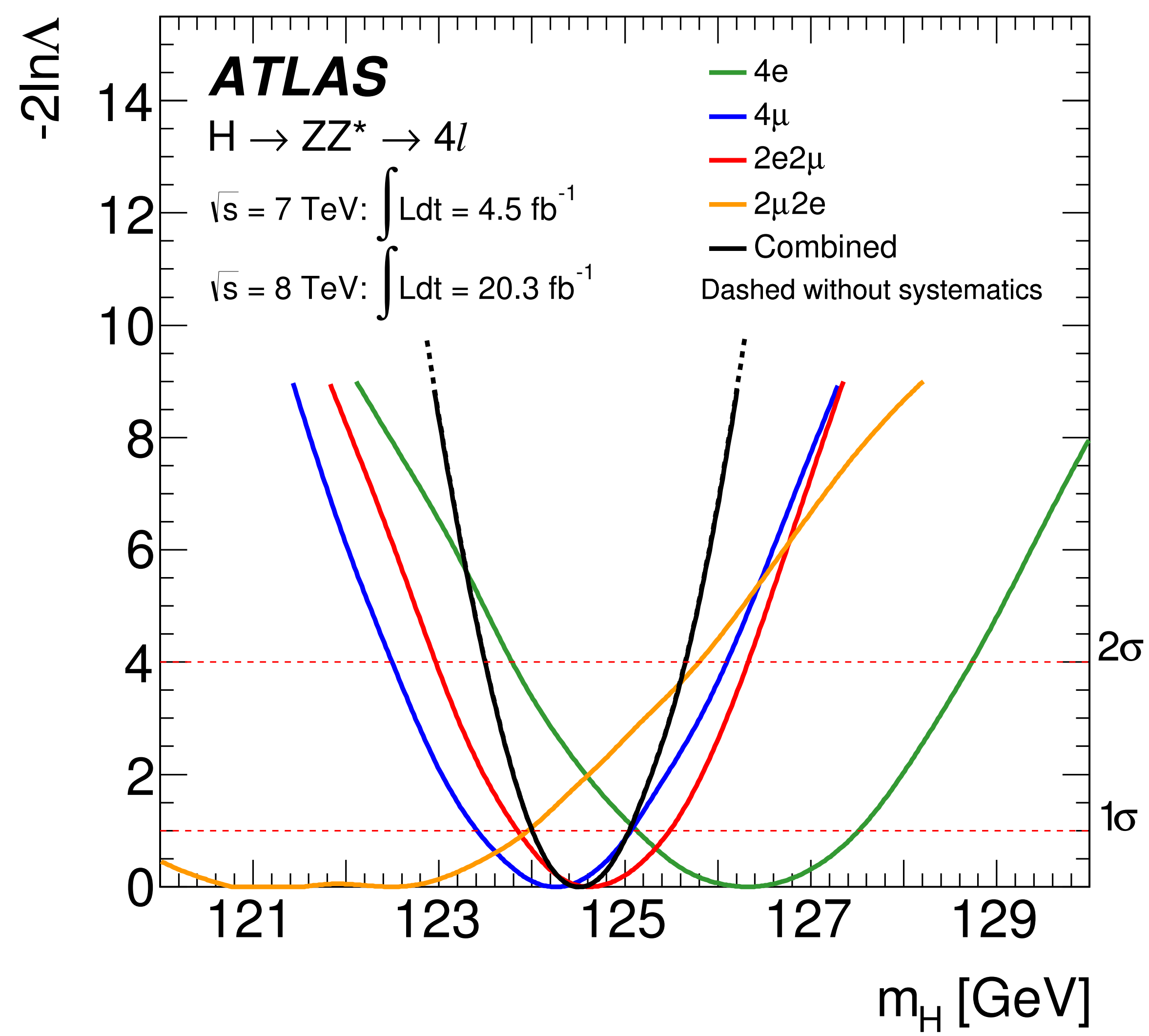

$m_H = 124.51 \pm 0.52\,(\text{stat}) \pm 0.06\,(\text{syst})$ GeV

previous result: $m_H = 124.3\,^{+0.6}_{-0.5}\,(\text{stat})\,^{+0.5}_{-0.3}\,(\text{syst})$ GeV

H→ZZ: indirect Γ_H measurement

$$\mu_{\text{on-shell}} = \frac{\kappa^2_{g,\text{on-shell}} \cdot \kappa^2_{V,\text{on-shell}}}{\Gamma_H/\Gamma_H^{\text{SM}}}$$

$$\frac{d\sigma_{pp\to H\to ZZ}}{dM^2_{4l}} \sim \frac{g^2_{Hgg}g^2_{HZZ}}{(M^2_{4l}-m^2_H)^2+m^2_H\Gamma^2_H}.$$

$$\mu_{\text{off-shell}} = \kappa^2_{g,\text{off-shell}} \cdot \kappa^2_{V,\text{off-shell}}$$

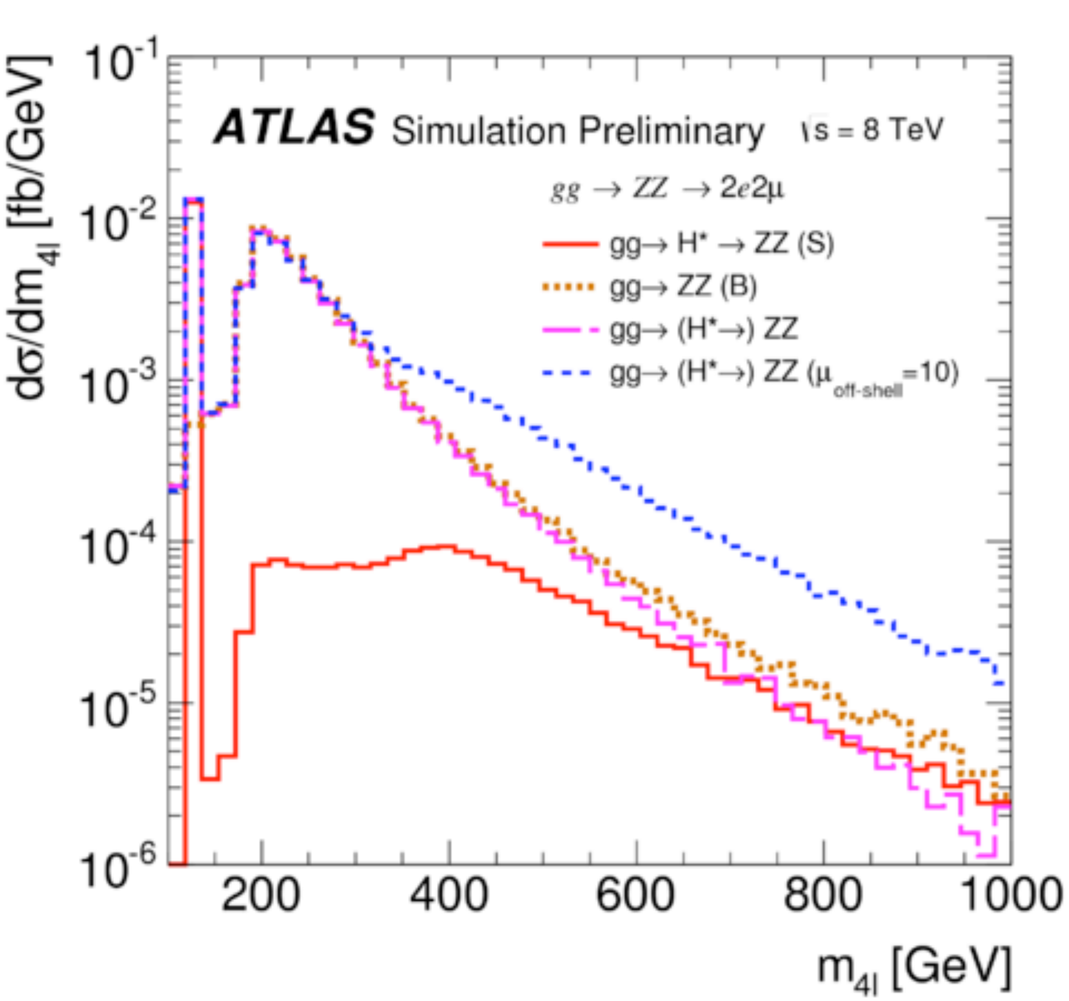

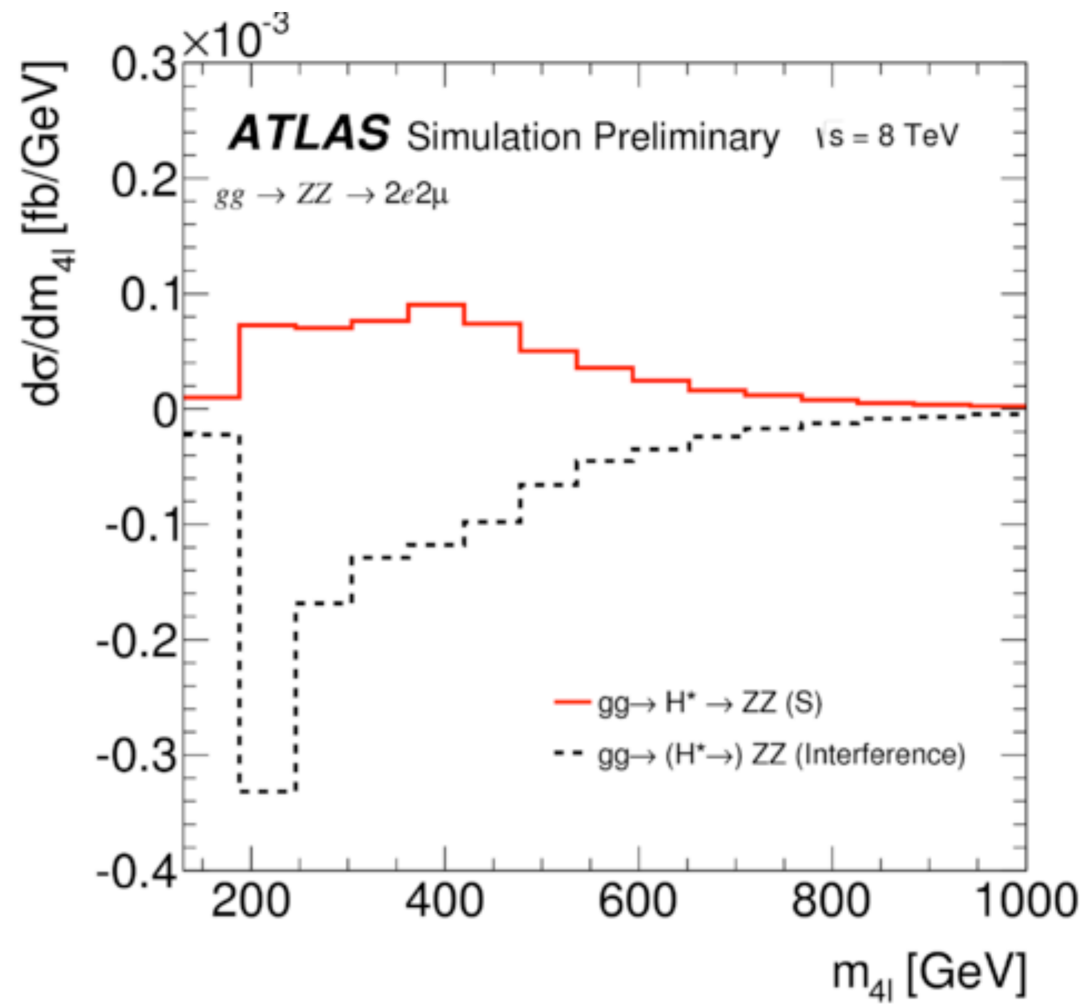

H→$\gamma\gamma$: Event categorization (1)

Table 1: Summary of the expected number of signal events in the 105–160 GeV mass range n_{sig}, the FWHM of mass resolution, σ_{eff} (half of the smallest range containing 68% of the signal events), number of background events b in the smallest mass window containing 90% of the signal (σ_{eff90}), and the ratio s/b and $s/\sqrt{b}$ with s the expected number of signal events in the window containing 90% of signal events, for the $H \to \gamma\gamma$ channel. b is derived from the fit of the data in the 105–160 GeV mass range. The value of m_H is taken to be 126 GeV and the signal yield is assumed to be the expected Standard Model value. The estimates are shown separately for the 7 TeV and 8 TeV datasets and for the inclusive sample as well as for each of the categories used in the analysis.

Category	n_{sig}	FWHM [GeV]	σ_{eff} [GeV]	b in $\pm\sigma_{\mathrm{eff90}}$	s/b [%]	$s/\sqrt{b}$
			$\sqrt{s}$=8 TeV			
Inclusive	402.	3.69	1.67	10670	3.39	3.50
Unconv. central low p_{Tt}	59.3	3.13	1.35	801	6.66	1.88
Unconv. central high p_{Tt}	7.1	2.81	1.21	26.0	24.6	1.26
Unconv. rest low p_{Tt}	96.2	3.49	1.53	2624	3.30	1.69
Unconv. rest high p_{Tt}	10.4	3.11	1.36	93.9	9.95	0.96
Unconv. transition	26.0	4.24	1.86	910	2.57	0.78
Conv. central low p_{Tt}	37.2	3.47	1.52	589	5.69	1.38
Conv. central high p_{Tt}	4.5	3.07	1.35	20.9	19.4	0.88
Conv. rest low p_{Tt}	107.2	4.23	1.88	3834	2.52	1.56
Conv. rest high p_{Tt}	11.9	3.71	1.64	144.2	7.44	0.89
Conv. transition	42.1	5.31	2.41	1977	1.92	0.85
			$\sqrt{s}$=7 TeV			
Inclusive	73.9	3.38	1.54	1752	3.80	1.59
Unconv. central low p_{Tt}	10.8	2.89	1.24	128	7.55	0.85
Unconv. central high p_{Tt}	1.2	2.59	1.11	3.7	30.0	0.58
Unconv. rest low p_{Tt}	16.5	3.09	1.35	363	4.08	0.78
Unconv. rest high p_{Tt}	1.8	2.78	1.21	13.6	11.6	0.43
Unconv. transition	4.5	3.65	1.61	125	3.21	0.36
Conv. central low p_{Tt}	7.1	3.28	1.44	105	6.06	0.62
Conv. central high p_{Tt}	0.8	2.87	1.25	3.5	21.6	0.40
Conv. rest low p_{Tt}	21.0	3.93	1.75	695	2.72	0.72
Conv. rest high p_{Tt}	2.2	3.43	1.51	24.7	7.98	0.40
Conv. transition	8.1	4.81	2.23	365	2.00	0.38

$H \rightarrow \gamma\gamma$: Event categorization (2)

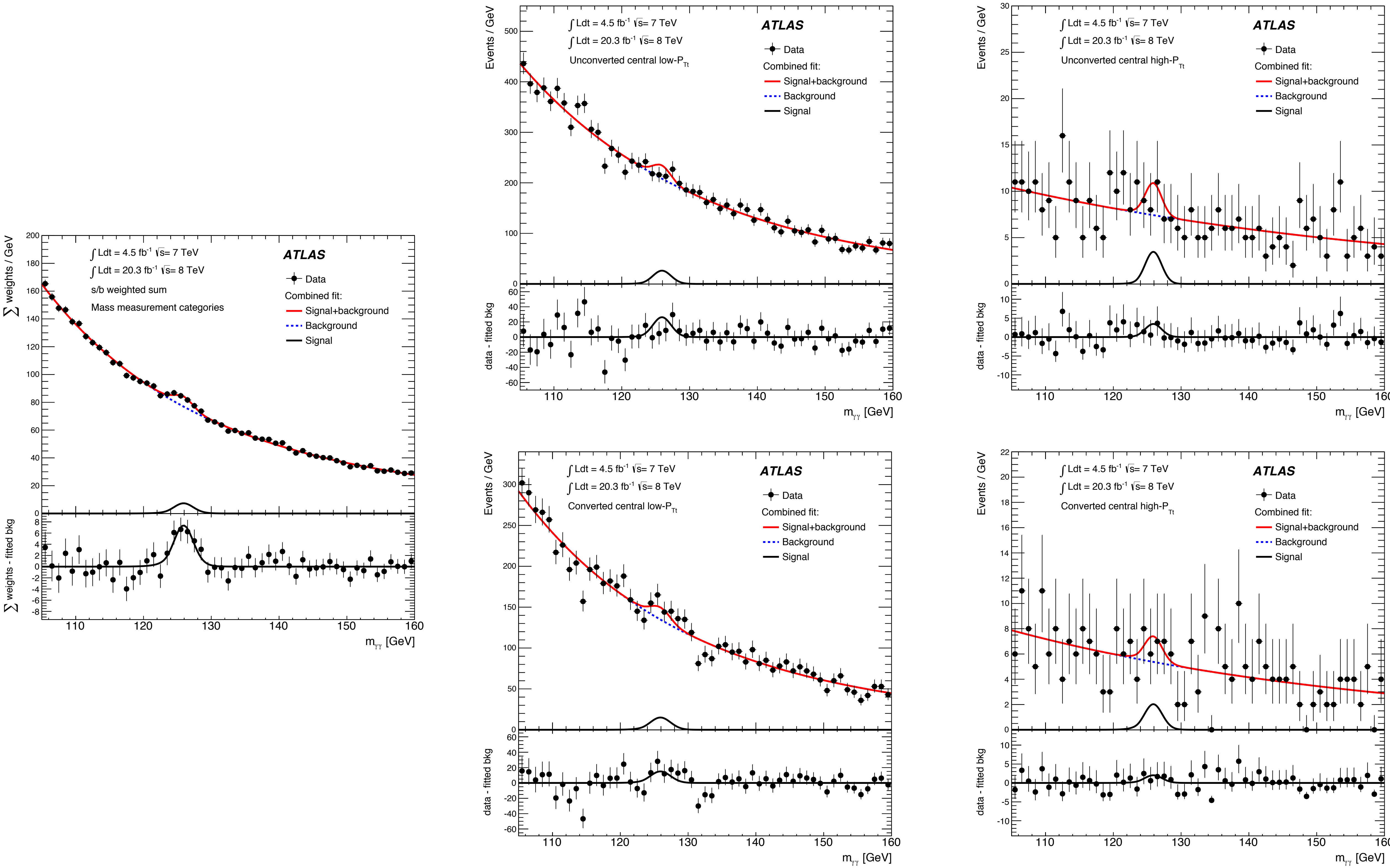

$H \rightarrow \gamma\gamma$: Mass measurement

- New result: 125.98 ± 0.42(stat) ± 0.28(syst) GeV
- Previous result: 126.8 ± 0.2 (stat) ± 0.7 (syst) GeV
  - Observed shift: 0.8 GeV / Expected change: -0.45 ± 0.35 GeV
    (consistent with expected change from updated photon energy scale calibration)
- Statistical error compatible with expected for given signal strength (p-value 16%)
  - Reduced with respect to the past because:
    - Reduced signal strength
    - Changes in mass resolution and event categorization
    - Consistent with a statistical fluctuation from changes in the measured masses of individual events

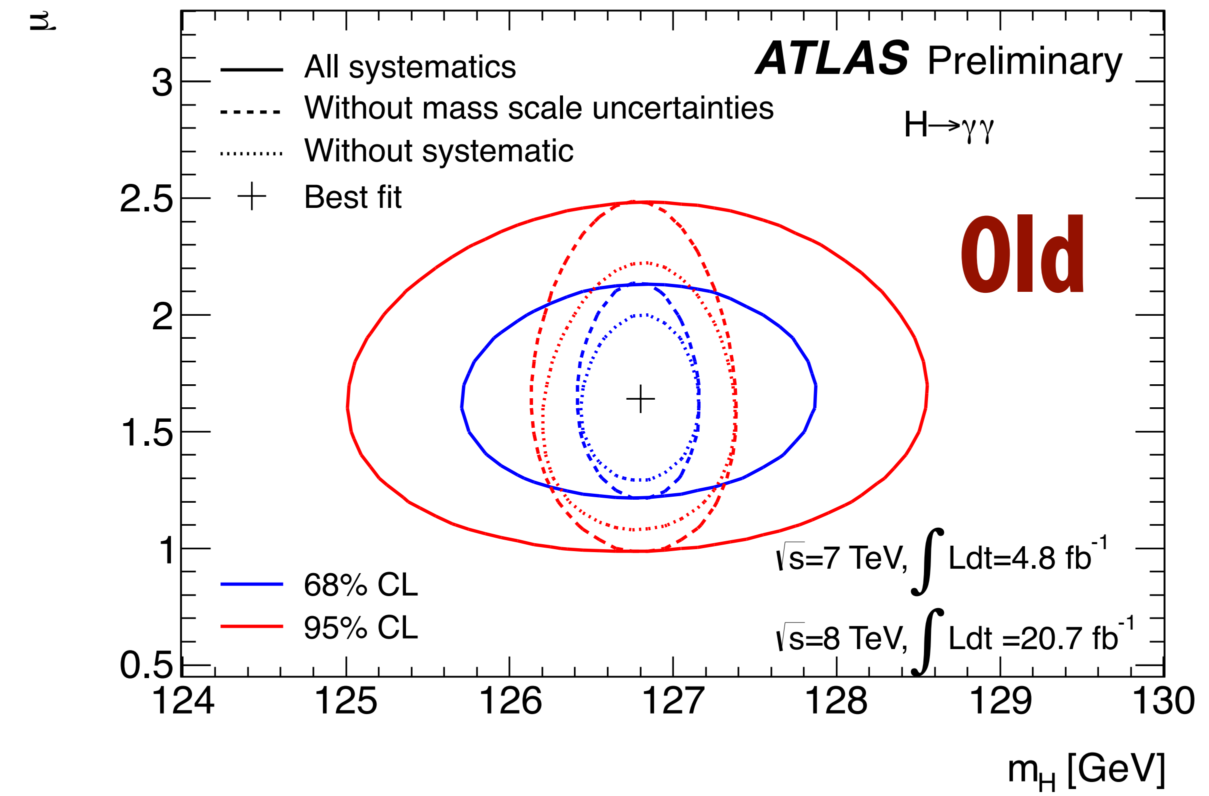

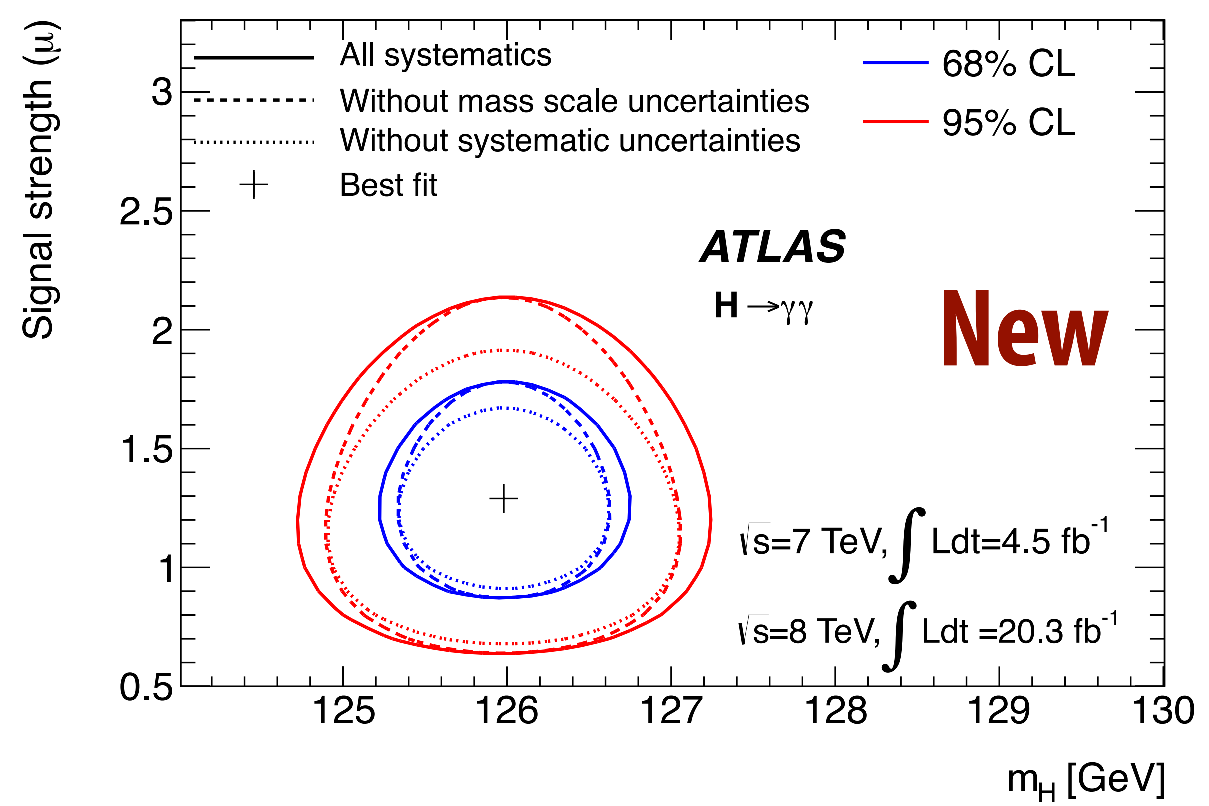

$H \rightarrow \gamma\gamma$: Mass measurement checks

- Many cross-checks performed:
  - Splitting events according to:
    - conversions
    - number of primary vertices
    - detector region
  - All checks consistent, no deviations above 1.5σ

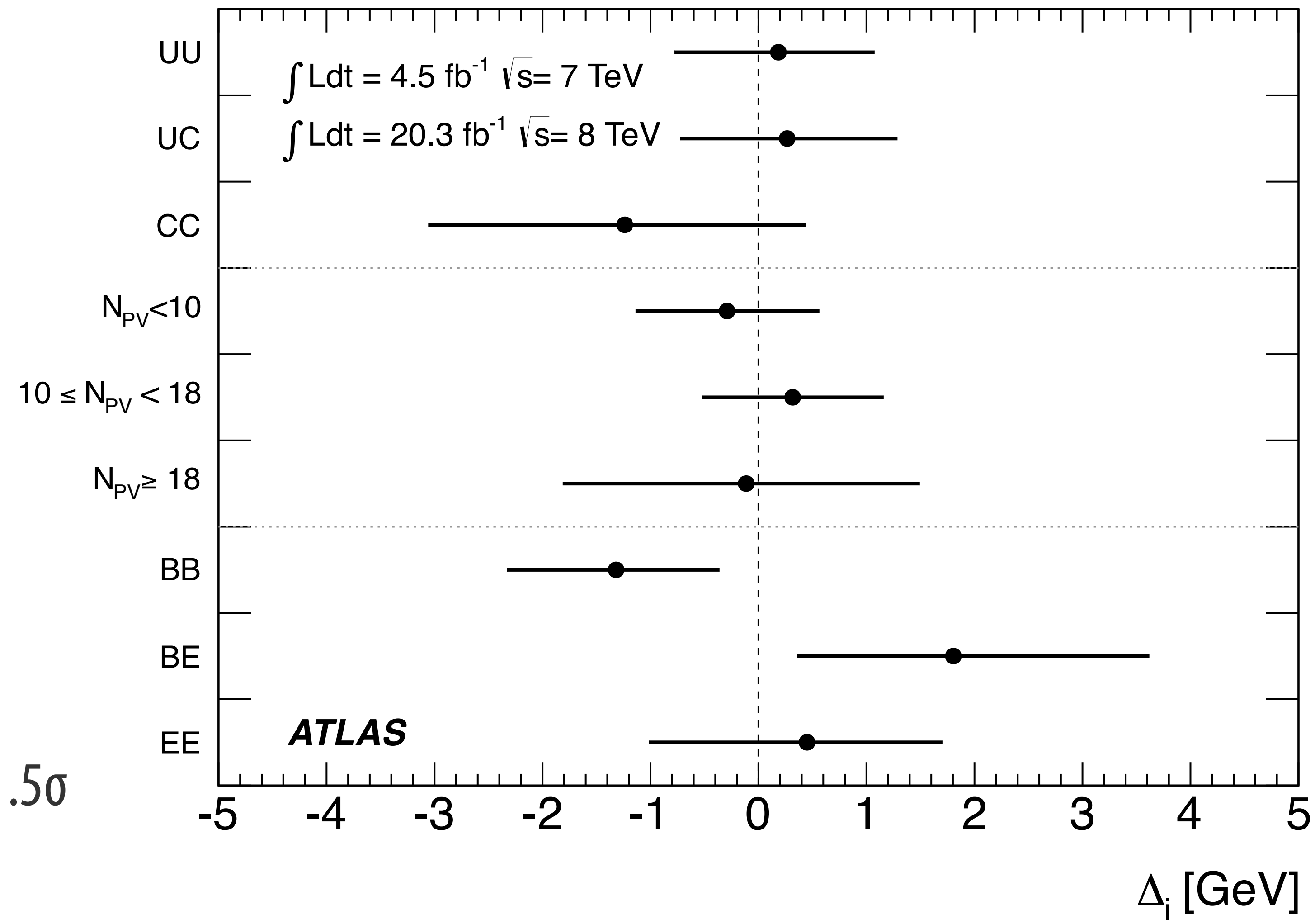

Mass measurement: systematics

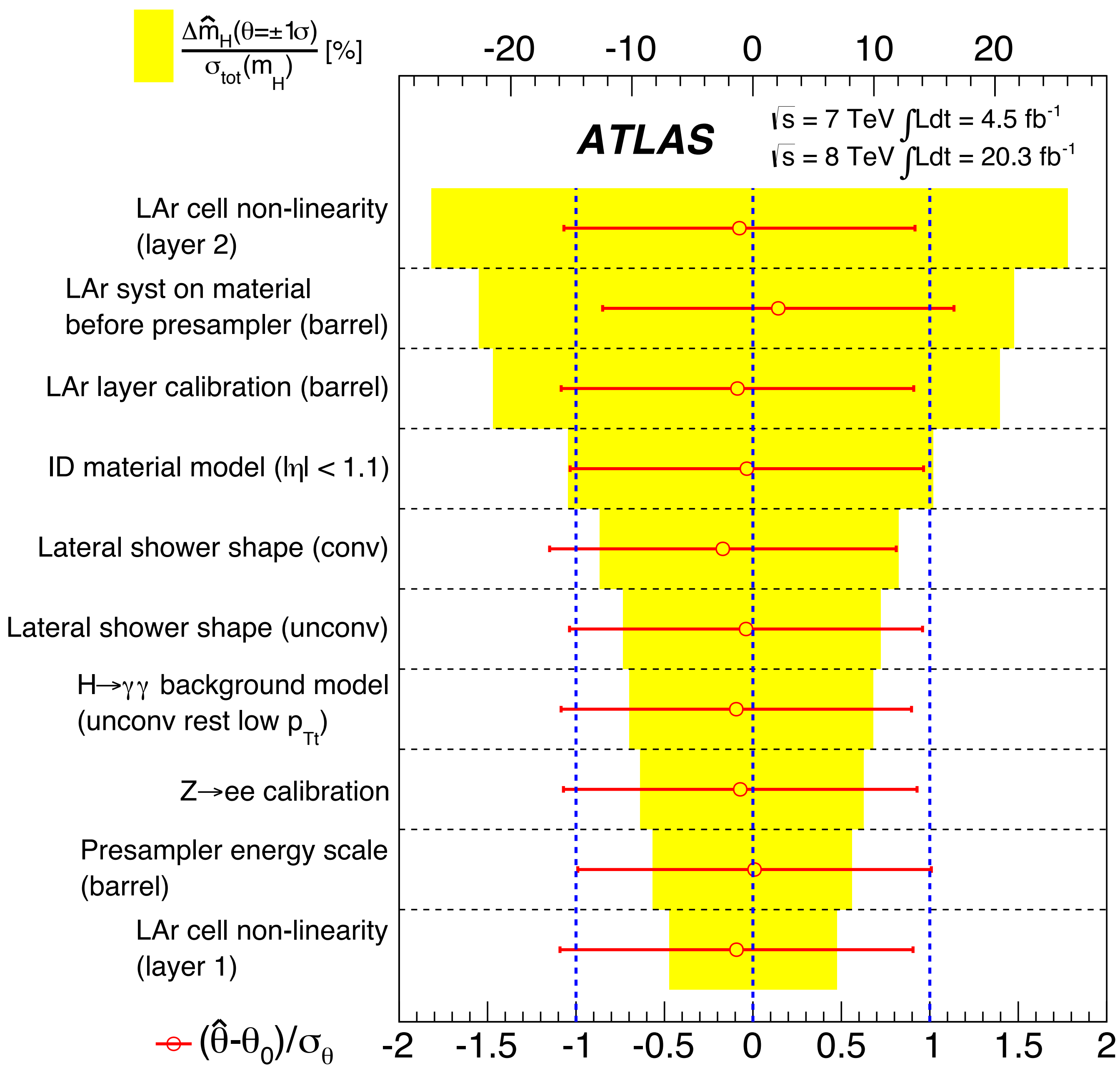

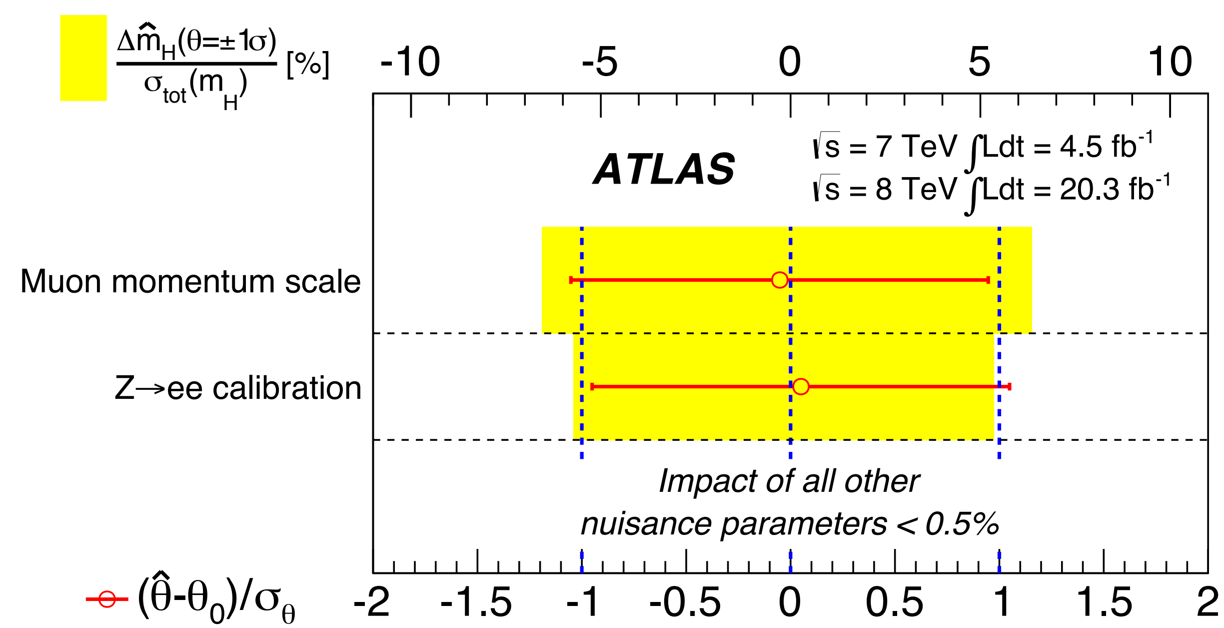

$H \rightarrow ZZ \rightarrow 4\ell$: cross section

- Based on the same event selection as used in the $H \rightarrow 4l$ mass and couplings measurements
  - Inclusive measurement
    - simple cut and count measurement using a mass window
    - more precise measurement based on a fit of the invariant mass distribution
  - Differential measurements
    - Higgs pT and rapidity, cos(θ*), M34, Njets, leading jet pT
    - only cut and count measurement using a mass window
- Estimate background yields (as in main analysis) and shapes
- Unfold reconstructed signal to truth distribution in fiducial volume
- Comparisons to different theory calculations

H→ZZ→4ℓ: cross section

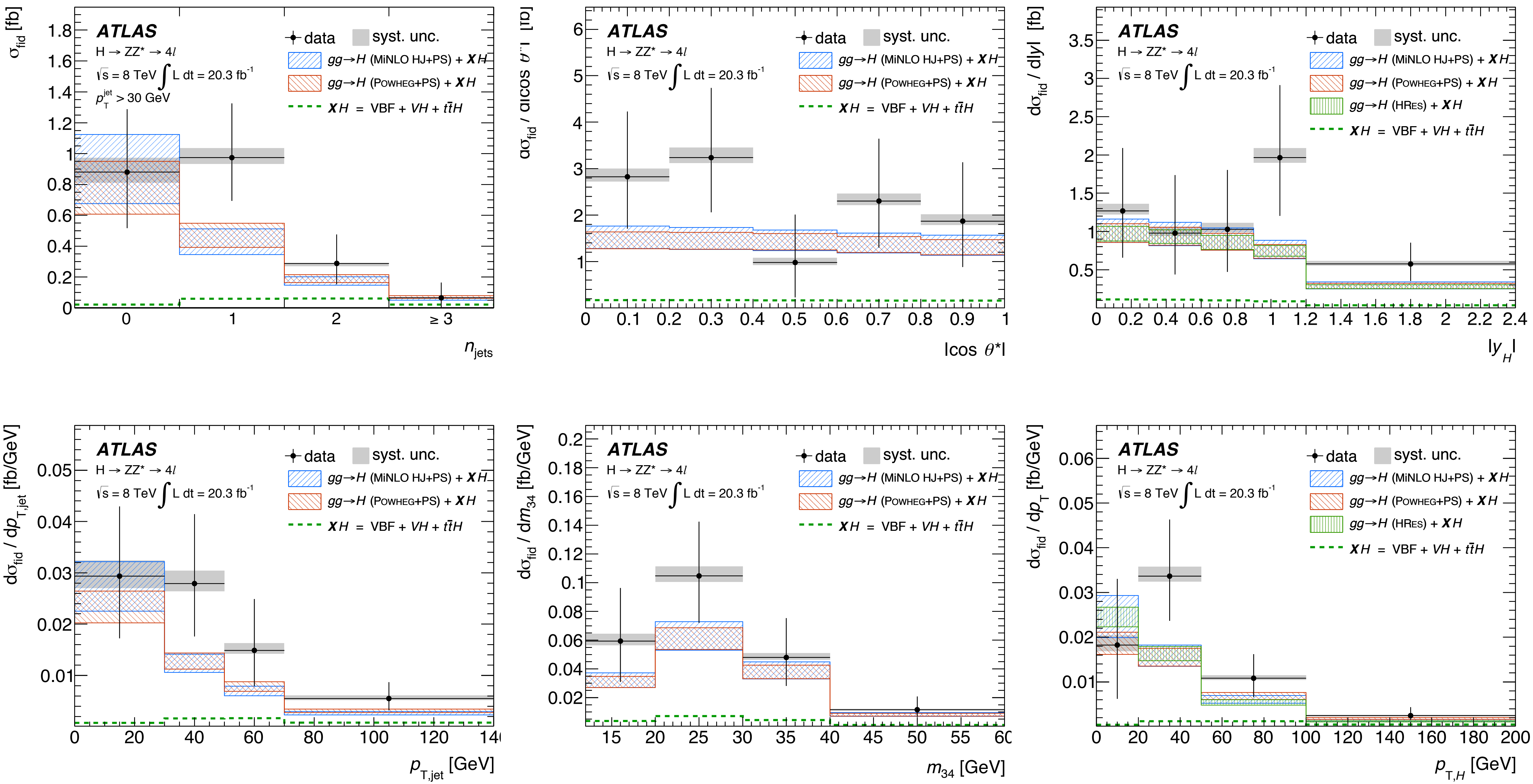

$H \to \gamma\gamma$: cross section

Fiducial region	N_{data}	$N_{\text{MC}}^{\text{sig}}$	ν_i^{sig}
Baseline	94627	403 ± 45	570 ± 130
$N_{\text{jets}} \geq 1$	34293	$178\,^{+31}_{-26}$	308 ± 79
$N_{\text{jets}} \geq 2$	10699	63 ± 11	141 ± 43
$N_{\text{jets}} \geq 3$	2840	17 ± 4	64 ± 22
VBF-enhanced	334	13 ± 2	24 ± 9
$N_{\text{leptons}} \geq 1$	168	3.5 ± 0.4	-3 ± 5
$E_{\text{T}}^{\text{miss}} > 80$ GeV	154	2.6 ± 0.4	-2 ± 4

Table 1. The total number of events selected in data in each fiducial region, N_{data}, the expected signal yield obtained from the simulation samples discussed in section 4, $N_{\text{MC}}^{\text{sig}}$, and the fitted yield obtained from data, ν_i^{sig}. The uncertainty on the fitted yield is the total uncertainty on the signal extraction, including the statistical and systematic uncertainties. The uncertainty on the expected yields include both the theoretical and experimental systematic uncertainties.

H→$\gamma\gamma$: cross section

Source	Uncertainty on fiducial cross section (%)				
	Baseline	$N_{\mathrm{jets}} \geq 1$	$N_{\mathrm{jets}} \geq 2$	$N_{\mathrm{jets}} \geq 3$	VBF-enhanced
Signal extraction (stat.)	± 22	± 25	± 30	± 33	± 34
Signal extraction (syst.)	± 6.5	± 7.4	± 7.1	± 6.5	± 9.0
Photon efficiency	± 1.5	± 2.1	± 3.1	± 4.2	± 2.3
Jet energy scale/resolution	-	${}^{+6.2}_{-5.8}$	${}^{+11}_{-10}$	${}^{+15}_{-13}$	${}^{+12}_{-11}$
JVF/pileup-jet	-	± 1.3	± 2.2	± 3.3	± 0.5
Theoretical modelling	${}^{+3.3}_{-1.0}$	${}^{+5.0}_{-2.6}$	± 4.1	${}^{+6.3}_{-4.9}$	${}^{+2.2}_{-3.2}$
Luminosity	± 2.8	± 2.8	± 2.8	± 2.8	± 2.8

Table 2. Uncertainties, expressed as percentages, on the cross sections measured in the baseline, $N_{\mathrm{jets}} \geq 1$, $N_{\mathrm{jets}} \geq 2$, $N_{\mathrm{jets}} \geq 3$ and VBF-enhanced fiducial regions. The signal extraction systematic uncertainty contains the effect of the photon energy scale and resolution, the impact of the background modelling on the signal yield and the uncertainty in the fitted peak position from the chosen background parameterisation.

H→ZZ→4ℓ: Couplings

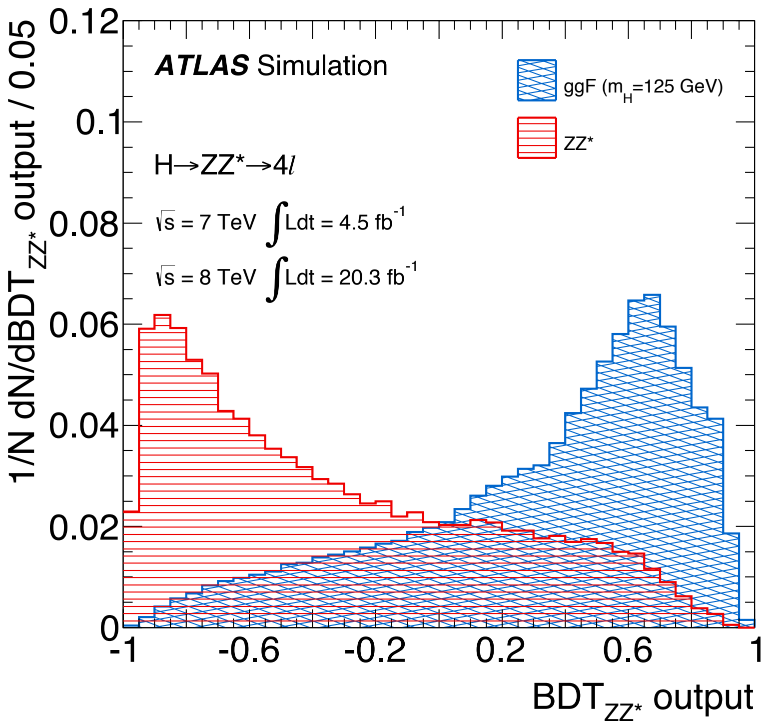

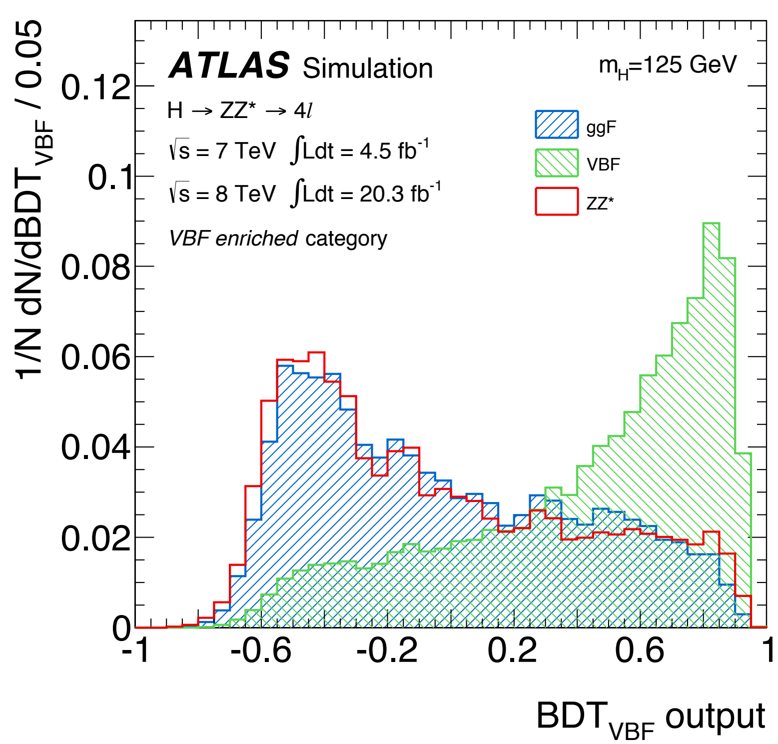

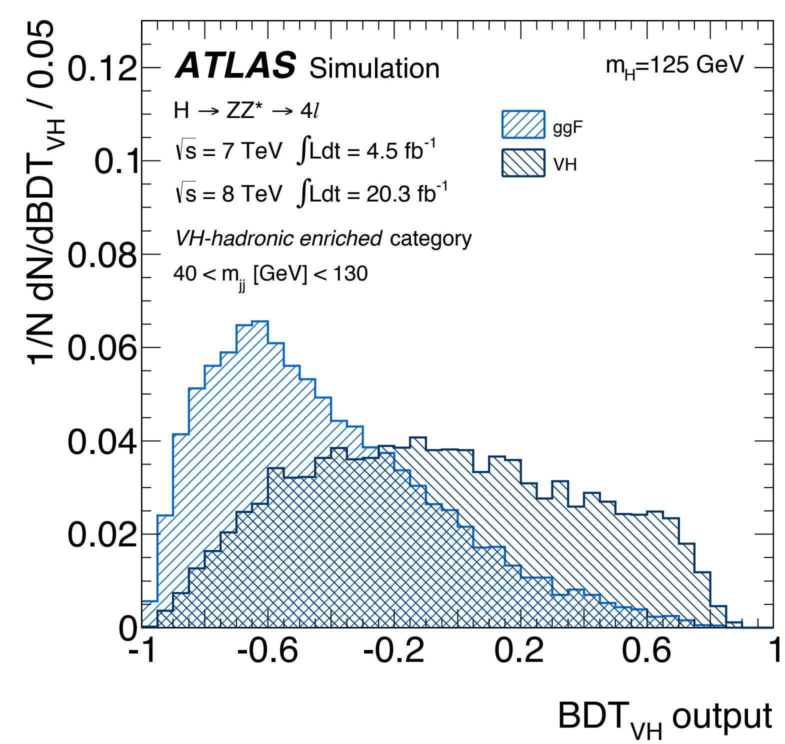

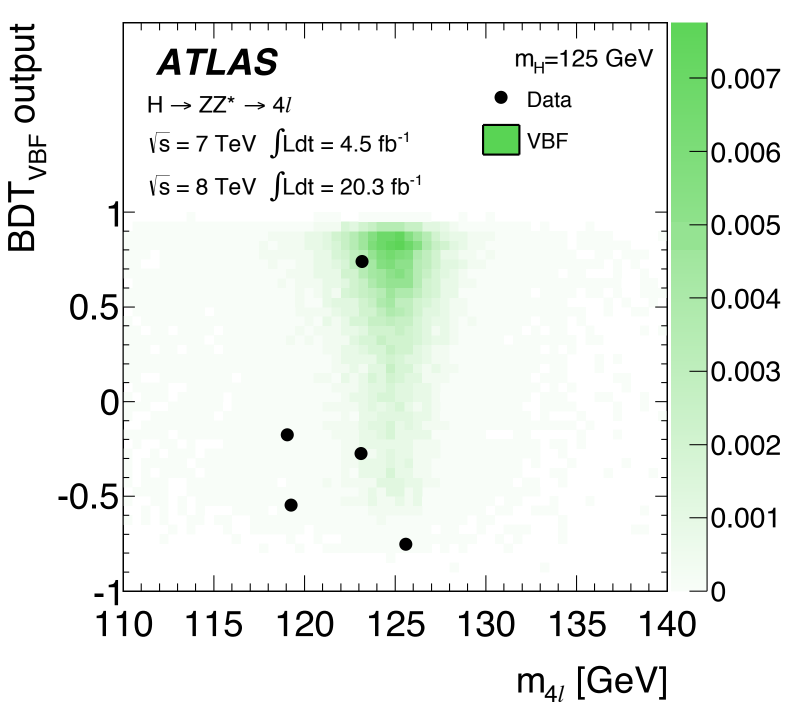

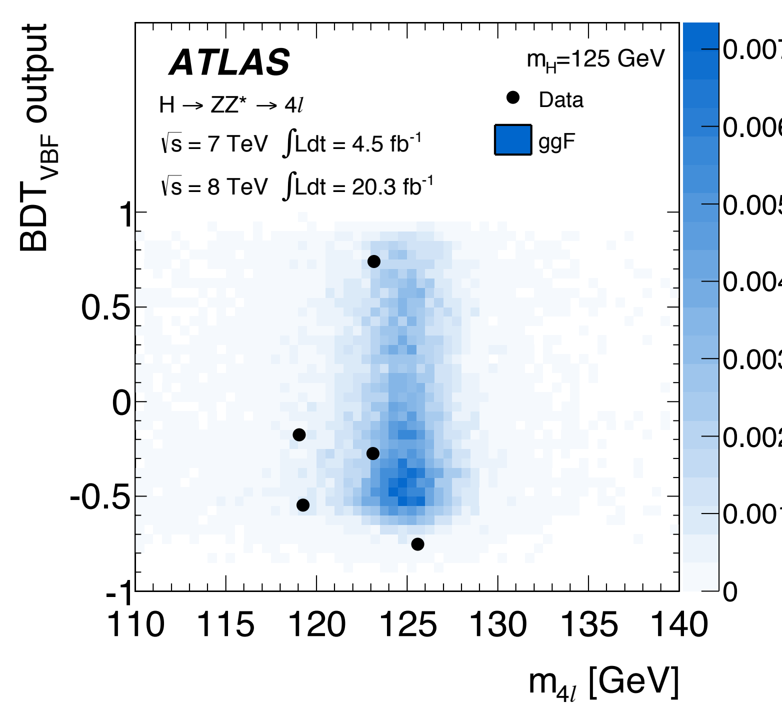

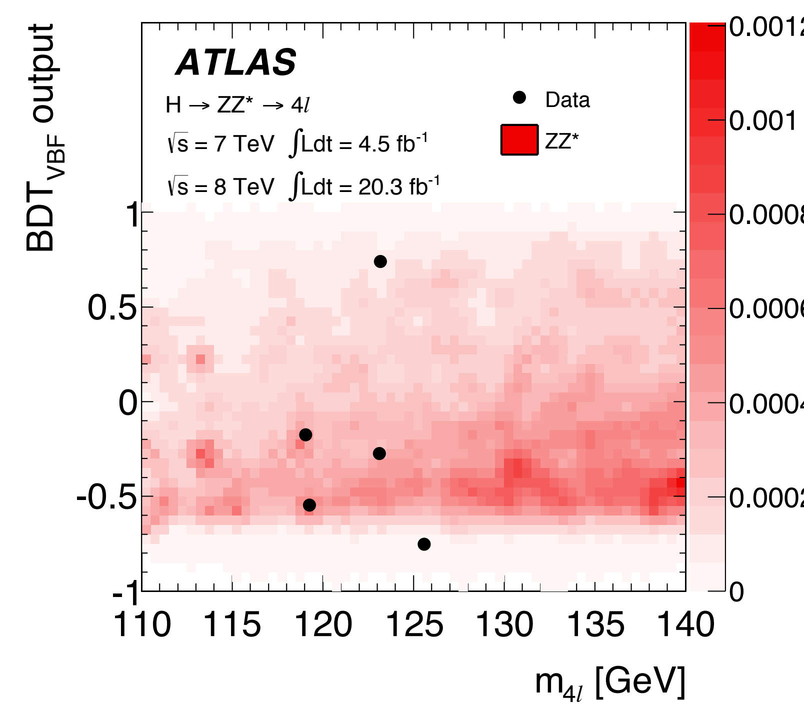

$H \to \gamma\gamma$: Couplings

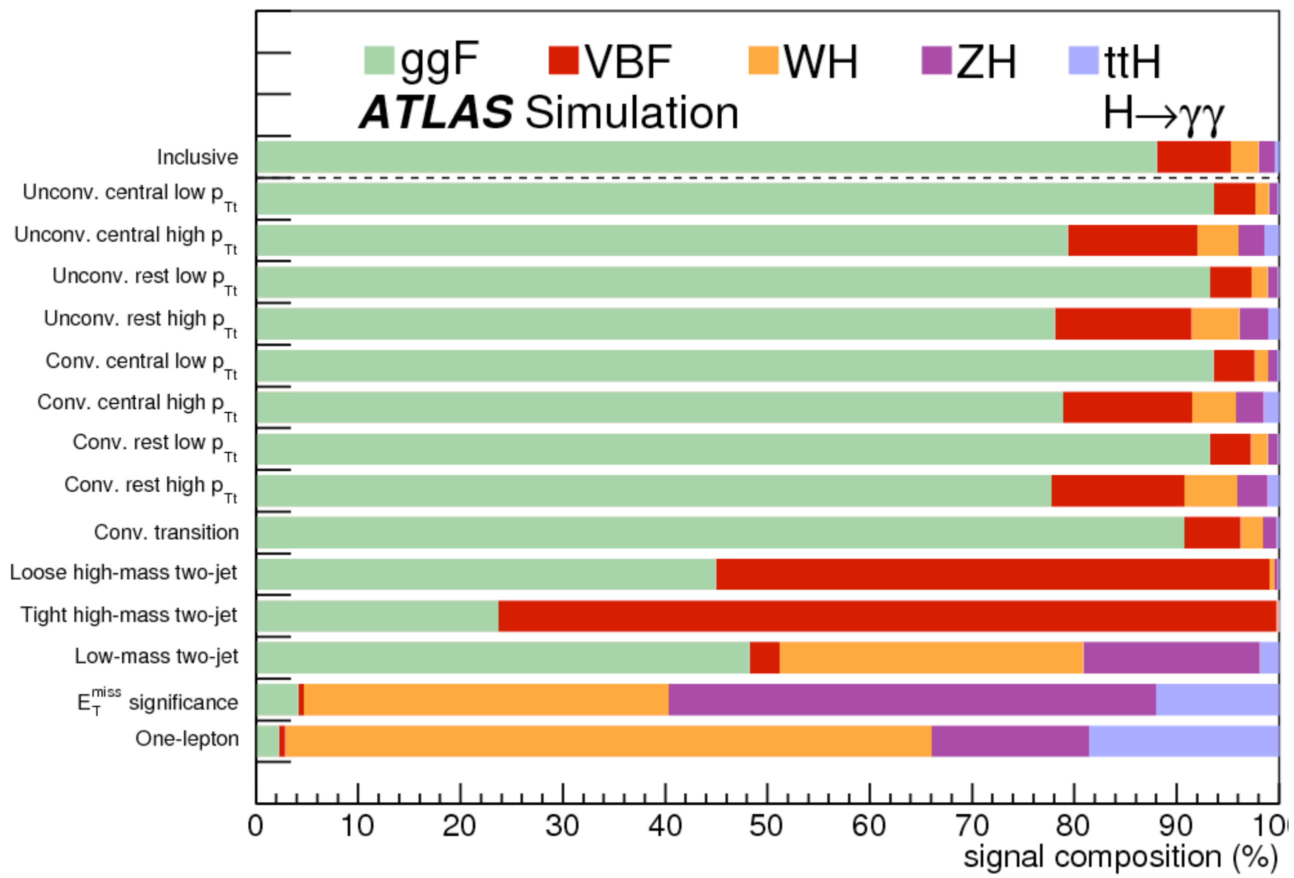

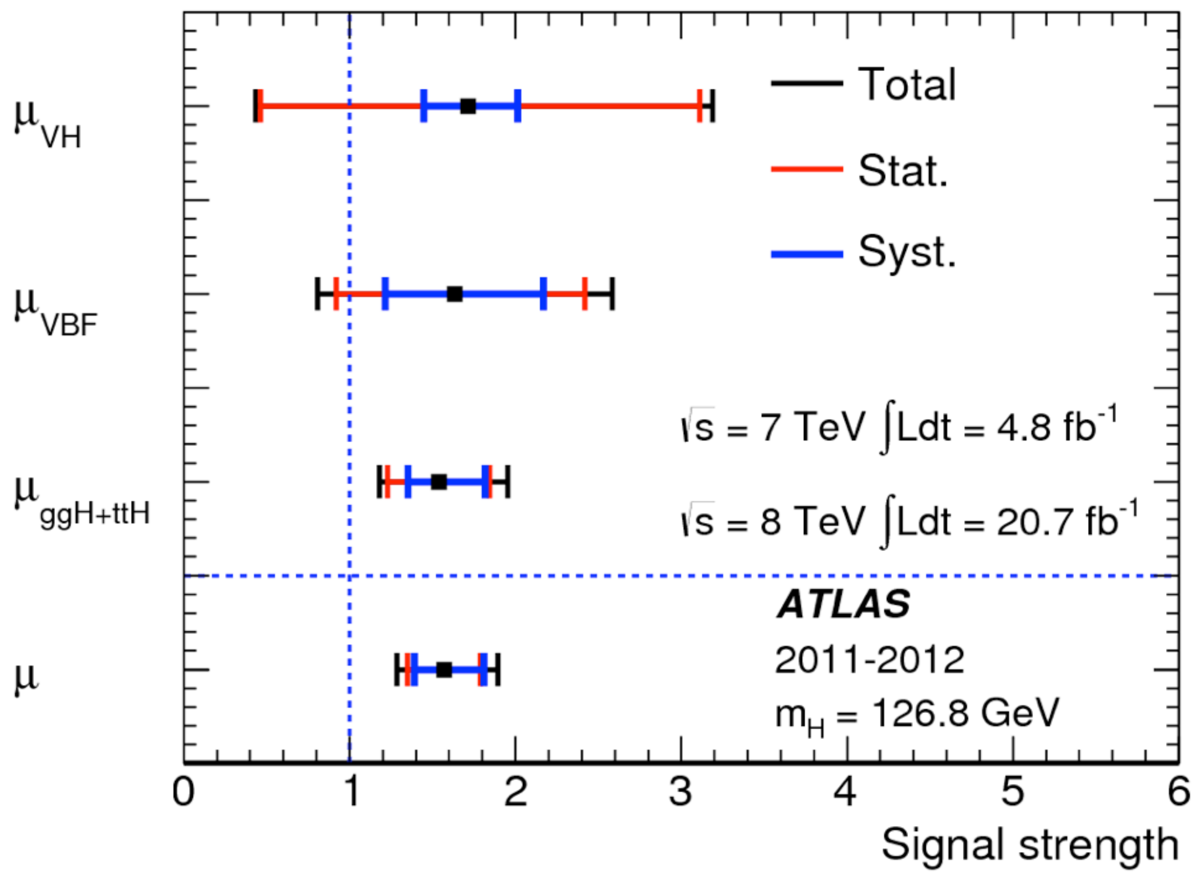

10.2.2 *Definition of coupling scale factors*

In order to take into account the currently best available SM predictions for Higgs cross sections, which include higher-order QCD and EW corrections [13, 14, 409], while at the same time introducing possible deviations from the SM values of the couplings, the predicted SM Higgs cross sections and partial decay widths are dressed with scale factors κ_i. The scale factors κ_i are defined in such a way that the cross sections σ_{ii} or the partial decay widths Γ_{ii} associated with the SM particle i scale with the factor κ_i^2

132

when compared to the corresponding SM prediction. Table 36 lists all relevant cases. Taking the process $gg \to H \to \gamma\gamma$ as an example, one would use as cross section:

$$(\sigma \cdot \mathrm{BR})\,(gg \to H \to \gamma\gamma) \quad = \quad \sigma_{\mathrm{SM}}(gg \to H) \cdot \mathrm{BR}_{\mathrm{SM}}(H \to \gamma\gamma) \cdot \frac{\kappa_g^2 \cdot \kappa_\gamma^2}{\kappa_H^2} \qquad (93)$$

Couplings combination